Wheat *TaSPL8* Modulates Leaf Angle Through Auxin and Brassinosteroid Signaling[1][OPEN]

Kaiye Liu,[a,b,c,2] Jie Cao,[a,b,c,2] Kuohai Yu,[a,b,c] Xinye Liu,[a,b,c] Yujiao Gao,[a,b,c] Qian Chen,[a,b,c] Wenjia Zhang,[a,b,c] Huiru Peng,[a,b,c] Jinkun Du,[a,b,c] Mingming Xin,[a,b,c] Zhaorong Hu,[a,b,c] Weilong Guo,[a,b,c] Vincenzo Rossi,[d] Zhongfu Ni,[a,b,c] Qixin Sun,[a,b,c] and Yingyin Yao[a,b,c,3,4]

[a]State Key Laboratory for Agrobiotechnology, China Agricultural University, Beijing, 100193, China
[b]Key Laboratory of Crop Heterosis and Utilization (Ministry of Education), China Agricultural University, Beijing, 100193, China
[c]Beijing Key Laboratory of Crop Genetic Improvement, China Agricultural University, Beijing, 100193, China
[d]Council for Agricultural Research and Economics, Research Centre for Cereal and Industrial Crops, I-24126 Bergamo, Italy

ORCID IDs: 0000-0003-0274-3978 (W.Z.); 0000-0003-4010-4165 (M.X.); 0000-0002-1815-648X (Z.H.); 0000-0001-5199-1359 (W.G.); 0000-0001-9746-2583 (V.R.); 0000-0003-4122-4118 (Y.Y.).

In grass crops, leaf angle is determined by development of the lamina joint, the tissue connecting the leaf blade and sheath, and is closely related to crop architecture and yield. In this study, we identified a mutant generated by fast neutron radiation that exhibited an erect leaf phenotype caused by defects in lamina joint development. Map-based cloning revealed that the gene *TaSPL8*, encoding a SQUAMOSA PROMOTER BINDING-LIKE (SPL) protein, is deleted in this mutant. *TaSPL8* knock-out mutants exhibit erect leaves due to loss of the lamina joint, compact architecture, and increased spike number especially in high planting density, suggesting similarity with its *LIGULESS1* homologs in maize (*Zea mays*) and rice (*Oryza sativa*). Hence, *LG1* could be a robust target for plant architecture improvement in grass species. Common wheat (*Triticum aestivum*, $2n = 6\times = 42$; BBAADD) is an allohexaploid containing A, B, and D subgenomes and the homeologous gene of *TaSPL8* from the D subgenome contributes to the length of the lamina joint to a greater extent than that from the A and B subgenomes. Comparison of the transcriptome between the *Taspl8* mutant and the wild type revealed that *TaSPL8* is involved in the activation of genes related to auxin and brassinosteroid pathways and cell elongation. TaSPL8 binds to the promoters of the *AUXIN RESPONSE FACTOR* gene and of the brassinosteroid biogenesis gene *CYP90D2* and activates their expression. These results indicate that *TaSPL8* might regulate lamina joint development through auxin signaling and the brassinosteroid biosynthesis pathway.

Leaf angle, defined as the inclination between the leaf blade midrib and the stem, directly influences canopy structure and consequentially affects yield (Mantilla-Perez and Salas Fernandez, 2017). Plants with erect leaves have an increased capacity to intercept light and higher photosynthetic efficiency, which results in improved grain filling (Sinclair and Sheehy, 1999). More efficient grain filling enables planting of larger populations with a greater leaf area index. Hence, using plants with more erect leaves generally improves the yield per unit of cultivated area (Pendleton et al., 1968; Duvick, 2005; Lee and Tollenaar, 2007; Lauer et al., 2012). For example, the maize (*Zea mays*) *liguleless2* mutant has erect leaves and produces 40% more grain than its counterpart with horizontal-type leaves due to the relative efficiency of CO_2 fixation per unit of incoming sunlight, which increases as the leaf angle decreases (Pendleton et al., 1968). In rice (*Oryza sativa*), the *Osdwarf4-1* mutant exhibits an erect leaf phenotype that is associated with brassinosteroid (BR) deficiency and has enhanced grain yields under dense planting populations (Sakamoto et al., 2006). In wheat (*Triticum* sp), the important characteristics of the ideal plant architecture (ideotype) include short and strong stems with few, small, and erect leaves (Donald, 1968). Wheat genotypes with erect leaves also have a superior net carbon fixation capacity during grain filling (Austin et al., 1976). Therefore, breeding grass crops for more erect leaves is a reasonable strategy for improving crop productivity.

[1]This work was supported by the National Key Research and Development Program of China (grant nos. 2016YFD0100801 and 2016YFD0101004).

[2]These authors contributed equally to this article.

[3]Author for contact: yingyin@cau.edu.cn.

[4]Senior author.

The author responsible for distribution of materials integral to the findings presented in this article in accordance with the policy described in the Instructions for Authors (www.plantphysiol.org) is: Yingyin Yao (yingyin@cau.edu.cn).

Z.N., Q.S., and Y.Y. conceived this project and designed all experiments; K.L., J.C., K.Y., X.L., Y.G., M.X., W.Z., and W.G. performed the experiments and data analysis; Q.C., H.P., and Z.H. contributed to the wheat transformation; Y.Y., V.R., and J.D. contributed to article writing and revision.

[OPEN]Articles can be viewed without a subscription.

www.plantphysiol.org/cgi/doi/10.1104/pp.19.00248

Leaf angle depends on cell division, expansion, and cell wall composition in the lamina joint (including the auricle and ligule), which connects the leaf blade and sheath (Kong et al., 2017; Zhou et al., 2017). Genetic and functional studies indicated that various factors are involved in regulating lamina joint development, and consequentially affect leaf angle. Phytohormones, such as BR and auxin, play crucial roles in regulating the lamina inclination (Luo et al., 2016). In rice, loss of function of BR biosynthetic genes, such as *dwarf4-1* (Sakamoto et al., 2006), *ebisu dwarf* (Hong et al., 2003), *brassinosteroid-deficient dwarf1* (*brd1*; Hong et al., 2002), and *chromosome segment deleted dwarf1* (Li et al., 2013) results in reduced leaf inclination. Lamina joint development is also associated with BR signaling, as reported by studies of mutants less sensitive to BR, such as the BR-defective mutant *d61* (Yamamuro et al., 2000) and transgenic rice plants with suppressed expression of *BRASSINOSTEROID INSENSITIVE1-Associated receptor Kinase1* (Li et al., 2009) and *BRASSINAZOLE-RESISTANT1* (Bai et al., 2007). Similarly, auxin biosynthesis and signaling pathways influence lamina joint development. Both the gain-of-function rice *LEAF INCLINATION1* (Zhao et al., 2013) mutant and plants overexpressing Gretchen Hagen3 acyl acid amido synthetases (GH3) family members, including *OsGH3-1*, *-2*, *-5*, and *-13* (Du et al., 2012; Zhao et al., 2013; Zhang et al., 2015), have reduced auxin levels and show an enlarged leaf angle due to stimulated cell elongation at the lamina joint region. Rice transgenic lines overexpressing the auxin-responsive factor *OsARF19* exhibit an enlarged lamina inclination related to the increase of adaxial cell division (Zhang et al., 2015). Furthermore, high concentrations of the auxin indole-3-acetic acid (IAA) influence leaf inclination by interacting with BR (Wada et al., 1981; Cao and Chen, 1995) and ethylene, which also participates in BR-induced leaf inclination (Jang et al., 2017). Therefore, crosstalk occurs between different phytohormones in regulating lamina joint development and leaf inclination.

Genetic approaches have identified several genes that affect lamina joint development in rice and maize (Mantilla-Perez and Salas Fernandez, 2017). For instance, rice *BRASSINOSTEROID UPREGULATED1-LIKE1*, encoding a typical basic helix-loop-helix (bHLH) transcription factor, is preferentially expressed in the lamina joint and affects leaf angle by controlling cell elongation (Jang et al., 2017). Similarly, overexpression or ectopic expression of other bHLH transcription factor genes, such as *LAX PANICLE*, *OsbHLH153*, *OsbHLH173*, *OsbHLH174*, *BRASSINOSTEROID UPREGULATED1*, *INCREASED LAMINA INCLINATION1*, and *POSITIVE REGULATOR OF GRAIN LENGTH1*, results in a larger lamina inclination (Komatsu et al., 2003; Tanaka et al., 2009; Zhang et al., 2009; Dong et al., 2018). LC2, a VIN3-like protein, regulates lamina inclination by repressing adaxial cell division in the collar region (Zhao et al., 2010). An *increased leaf angle1* mutant shows increased leaf angle due to abnormal vascular bundle formation and cell wall composition in the lamina joint (Ning et al., 2011). It was suggested that rice SPX1, named after the suppressor of yeast *gpa1*, yeast cyclin-dependent kinase inhibitor, and human xenotropic and polytropic retrovirus receptor 1 (*SYG1/Pho81/XPR1*), could interact with Regulator of Leaf Inclination1 and negatively regulate leaf inclination by affecting lamina joint cell elongation (Ruan et al., 2018). Mutations in *LIGULELESS1* (*LG1*), which encodes a conserved SQUAMOSA PROMOTER BINDING-LIKE (SPL) transcription factor in maize and rice, result in an erect leaf phenotype with a complete loss of the auricle and ligule (Moreno et al., 1997; Lee et al., 2007). A single-nucleotide polymorphism in the upstream region of *OsLG1* may be responsible for its expression and affects panicle closure or spreading by controlling cell proliferation at the panicle pulvinus (Ishii et al., 2013; Zhu et al., 2013). However, the contributions of *LG1* to potential yield and its mechanism in affecting lamina joint development are still unknown.

In wheat, genetic approaches have identified several quantitative trait loci (QTL) that control leaf inclination. For example, QTL analysis of the markers for flag leaf angle from durum wheat (*Triticum durum*) populations indicated the presence of large-effect QTL on chromosomes 2A, 2B, 3A, 3B, 4B, 5B, and 7A (Isidro et al., 2012). Several environmentally stable QTL for flag leaf angle were mapped on chromosomes 1B, 3D, 5A, 6B, 7B, and 7D using two recombinant inbred line populations (Wu et al., 2015; Liu et al., 2018b). However, to date, no genes have been shown to be directly involved in the control of leaf angle in wheat. In this study, we characterized a common wheat (*Triticum aestivum*) mutant with a multigene deleted region, which exhibits erect leaves and compact plant architecture. We demonstrate that the *TaSPL8* gene, which encodes a SQUAMOSA PROMOTER BINDING-LIKE (SPL) protein and is homologous to *LG1* in maize and rice, is responsible for this mutant phenotype. Our results indicate that TaSPL8 regulates lamina joint development through affecting auxin response and BR biogenesis pathways, thus providing information about the mechanisms linking the activity of SPL family members and hormone-mediated regulation of leaf angle.

RESULTS

The *cpa* Mutant Exhibits Defects in Lamina Joint Development

To study the molecular mechanism that controls leaf angle in wheat, we screened for mutants with erect leaves from a wheat population mutagenized by fast neutron radiation. We identified a mutant, named *compact plant architecture* (*cpa*), with a smaller leaf angle and a more-compact plant architecture compared to wheat cultivar Liaochun10 (LC10; Fig. 1A). We measured the flag leaf angle between the midrib of the flag leaf and the internode below the spike in the *cpa* mutant and LC10 and found that the flag leaf angle was 11.50° and 28.23° in the *cpa* mutant and LC10, respectively (Fig. 1, B and

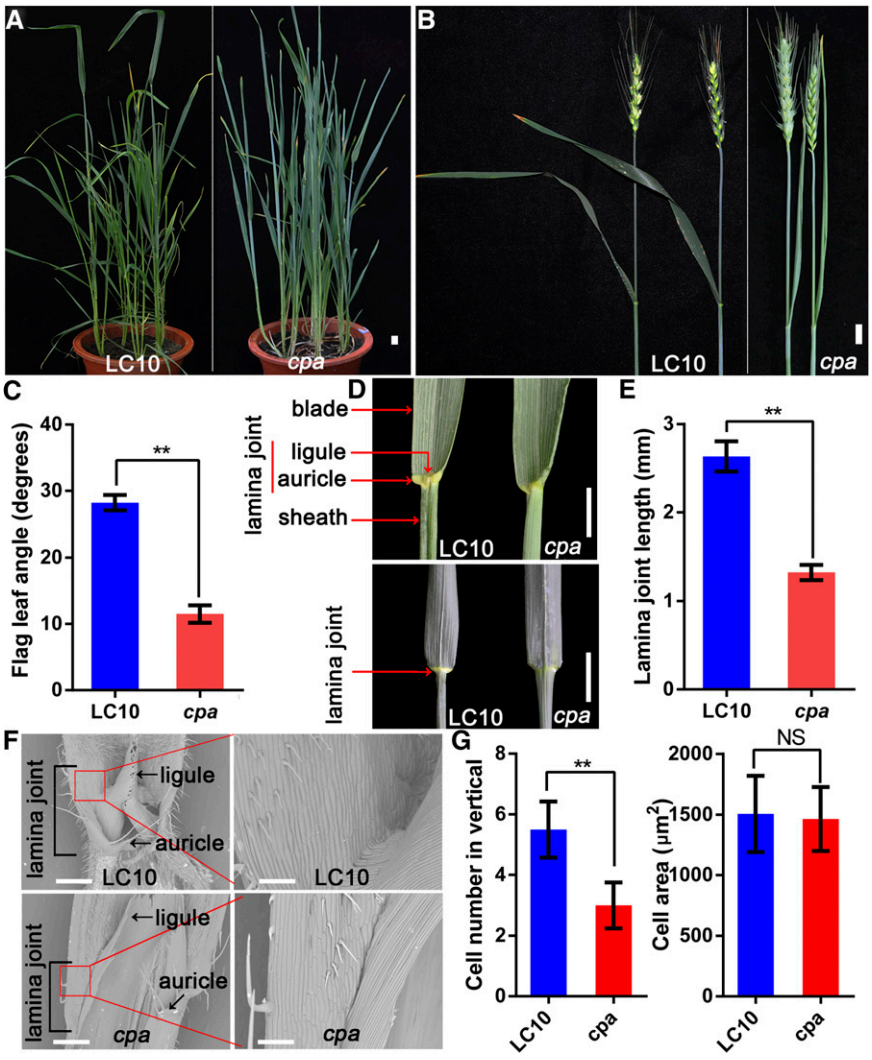

Figure 1. Morphological comparison of the wheat cultivar LC10 and the *cpa* mutant. A, Morphologies of LC10 and *cpa* plants at the heading stage. Bar = 2 cm. B, Morphologies of the flag leaf in LC10 and *cpa* plants at the flowering stage. Bar = 2 cm. C, Flag leaf angle of LC10 and *cpa* plants at the flowering stage. The double asterisk represents significant differences determined by the two-tailed Student's *t* test at $P < 0.01$. Error bars = SD ($n = 10$). D, The lamina joint phenotype of LC10 and *cpa* plants. Bars = 2 cm. E, Lamina joint length of LC10 and *cpa* plants. The double asterisk represents significant differences determined by two-tailed Student's *t* test at $P < 0.01$. Error bars = SD ($n = 10$). F, Morphology of the adaxial surface by a scanning electron microscope of the lamina joint of the LC10 and *cpa* flag leaf. Image magnification of the red box in the left (Bars = 200 μm) is shown on the right (Bars = 60 μm). G, Quantitative cell number and cell size of lamina joint from LC10 and *cpa* flag leaf. The cell number from the bottom to the top of the lamina joint was counted manually ($n = 10$) and cell size measured by the software ImageJ ($n = 15$). The double asterisk represents significant differences determined by two-tailed Student's *t* test at $P < 0.01$. Error bars = SD. NS, not significant.

C). The smaller flag leaf angle of the *cpa* mutant is mainly caused by abnormal development of the lamina joint (Fig. 1D). In particular, the length of the lamina joint of the flag leaf in the *cpa* mutant is 1.33 mm, whereas in LC10 it is 2.64 mm (Fig. 1E). Further morphological observation through scanning electron microscopy showed that the lamina joint is much smaller in the *cpa* mutant than in LC10 due to a decrease in cell number, although no changes in cell size were detected (Fig. 1, F and G). These results indicate that the *cpa* mutant exhibits defects in lamina joint development.

Map-Based Cloning of Mutated Gene

A genetic linkage analysis of 450 F2 individuals derived from a cross between LC10 and the *cpa* mutant was performed. A total of 335 individual plants showed a large lamina joint like LC10, while 115 plants showed a small lamina joint like the *cpa* mutant. This result indicated that the lamina joint defect of the *cpa* mutant is caused by a single recessive gene with a segregation ratio of approximately 3:1 ($\chi^2 = 0.074 < \chi^{2[0.05,1]} = 3.84$) of the normal phenotype versus the mutant phenotype. We designated the dominant wild-type gene as *TaCPA*.

Following a map-based cloning approach using 450 F2 individuals, *TaCPA* was found to cosegregate with markers *2D-235*, *2D1377*, *LMC-3*, and *2D-173* on chromosome 2D (Fig. 2A). By a larger segregation population consisting of 8,352 individuals we narrowed down the candidate region of *TaCPA* to ~19 Mb between *LMC-3* and *2D-173* (Fig. 2, B and C). Generation of additional markers in this region allowed the mapping of *TaCPA* as being completely linked to *LMC-15*, *-18*, *-19*, *-23*, *-60*, *-71*, and *-98* (Fig. 2, B and C). Near-isogenic lines (NILs) in the *cpa* genetic background containing the LC10 allele (NIL^{LC10}) and NILs in the LC10 genetic background containing the *cpa* allele (NIL^{cpa}) were generated through backcrossing of heterozygous F1 plants to LC10 and the *cpa* mutant for three generations (BC_3), respectively (Supplemental Fig. S1). The backcrossed line containing a heterozygous fragment from markers *LMC-3* and *2D-173* was selected. We found that in NIL^{LC10} plants, the flag leaf angle and lamina

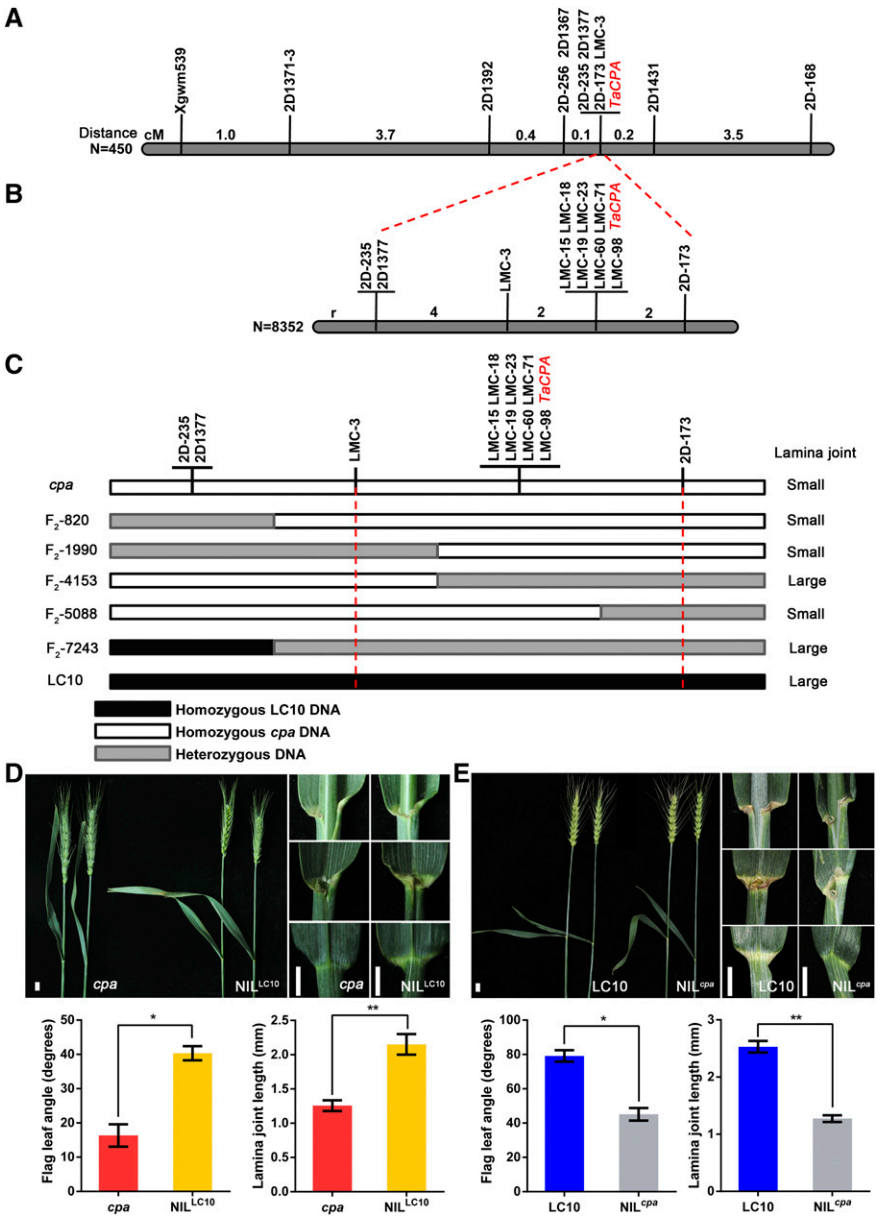

Figure 2. Fine mapping of the *TaCPA* locus and complementation test using NILs. A, Coarse linkage map of *TaCPA* on chromosome 2D. Numbers indicate the genetic distance between the adjacent markers. Thick black line indicates partial region of 2D chromosome. B, High-resolution linkage map of *TaCPA*. The number of recombinants (labeled as "r") between the molecular markers and *TaCPA* is indicated. Thick black line indicates partial region of 2D chromosome. C, Fine mapping of *TaCPA*. Genotypes and phenotypes of recombinants of five F2 plants including (F2-820, F2-1990, F2-4153, F2-5088, and F2-7243) are reported. The name and phenotype of F2 individual plants were labeled in the left and right parts, respectively. Black and white blocks indicate genomic region from LC10 and *cpa*, respectively. Gray blocks indicate the heterozygous region. D and E, Phenotype of the flag leaf angle and lamina joint in *cpa* and NIL^{LC10} (D) and NIL^{cpa} (E) plants. Bars = 1 cm. Single and double asterisks represent statistically significant differences determined by the two-tailed Student's *t* test at $P < 0.05$ and $P < 0.01$, respectively. Error bars = SD ($n = 10$).

joint length is significantly increased compared to the *cpa* mutant (Fig. 2D), while these parameters are decreased in the NIL^{cpa} plants compared to LC10 (Fig. 2E). This confirmed that *TaCPA* is located in the interval we have identified.

The region between markers *LMC-3* and *2D-173* contains a total of 257 predicted genes in the wheat Chinese Spring inbred line genome IWGSCv1(Appels et al., 2018). To map *TaCPA* at a higher resolution, we performed bulked segregant RNA sequencing (RNA-Seq), which makes use of the quantitative reads of RNA-Seq to efficiently map genes (Liu et al., 2012). RNA samples were extracted from 30 homozygous F2-derived F_3 lines with normal or mutant phenotypes and from *cpa* and LC10 plants and were combined into four separate pools used for RNA-Seq. Reads located in the region between markers *LMC-3* and *2D-173* were analyzed and the results indicated that 83 genes, distributed within this region, were expressed in both LC10 and homozygous normal phenotype pools, but were absent in the *cpa* mutant and mutant phenotype pools. These 83 genes could have been deleted in the *cpa* mutant by fast neutron radiation. To test this hypothesis, 10 genes located within and two genes located outside of the region (*LMC-3* to *2D-173*) were randomly selected and subjected to PCR amplification using genomic DNA of *cpa* and LC10 plants (Supplemental Fig. S2A). We found that all 10 genes within the *LMC-3-2D-173* region are absent in the *cpa* genome, while the two external genes are present (Supplemental Fig. S2B). The specificity of the primers used for the experiments was further assessed using Chinese Spring null-tetrasomic lines. PCR products were not obtained in the lines with a chromosome 2D deletion, but were present

in the other null-tetrasomic lines (Supplemental Fig. S2B). These results indicate that the chromosome fragment containing *TaCPA* is deleted in the *cpa* mutant.

TaSPL8, the Homolog of *LG1* in Maize and Rice, Affects Lamina Joint Development and Plant Architecture in Wheat

Among the 83 genes deleted in the *cpa* mutant, one gene (*TraesCS2D01G502900*), containing three exons and two introns, encodes a plant-specific SPL domain-containing transcription factor, SPL, with a total protein length of 407 amino acids. *TraesCS2D01G502900* shows high amino acid similarity to *OsLG1*(*SPL8*) in rice, *ZmLG1* in maize, and *SbLG1* in sorghum (*Sorghum bicolor*; Fig. 3A), which are involved in controlling auricle, ligule, and lamina joint development (Moreno et al., 1997; Lee et al., 2007). Therefore, we renamed *TaCPA* as *TaSPL8*, a candidate gene for lamina joint development in wheat. The expression of *TaSPL8* in various wheat tissues were detected by reverse transcription quantitative PCR (RT-qPCR), and we found that the *TaSPL8* transcript is highly expressed in the lamina joint and young spikes (Fig. 3B).

Wheat is a hexaploid species that possesses three subgenomes originating from the fusion of genomes from three diploid ancestral species (*Triticum urartu*, *Aegilops speltoides*, and *Aegilops tauschii*; El Baidouri et al., 2017). Accordingly, three *TaSPL8* homeologs were identified from the International Wheat Genome Sequencing Consortium database (IWGSCv1; Appels et al., 2018) and were designated *TaSPL8-2A*, *TaSPL8-2B*, and *TaSPL8-2D*, respectively. To determine whether the loss of *TaSPL8-2D* is responsible for the *cpa* mutant phenotype, we knocked out this gene using the

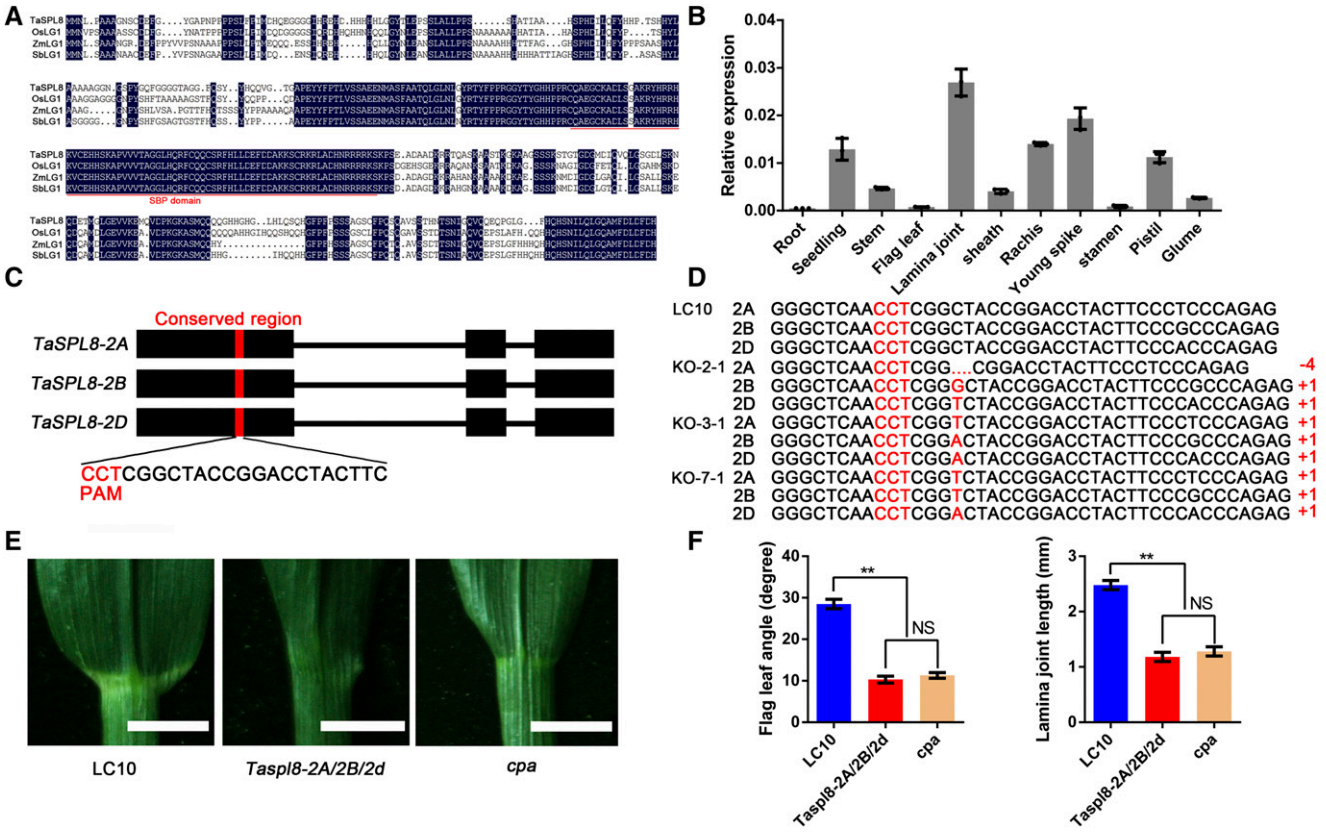

Figure 3. Cloning and characterization of *TaSPL8* and the phenotype of its knockout (KO) lines by the clustered regularly interspaced short palindromic repeats (CRISPR)/CRISPR-associated protein9 (Cas9) system. A, Amino acid sequence alignment of TaSPL8 and its orthologs in rice (Os04g0656500), maize (Zm00001d002005), and sorghum (SORBI_3006G247700). The conserved SQUAMOSA-PROMOTER BINDING PROTEIN domain is indicated by a red line. B, Expression pattern of *TaSPL8* in various tissues. The expression levels were normalized to wheat *TaACTIN*. Each bar in the graph corresponds to the mean value of three data points, shown by dots. C, Sequence of a single-guide RNA (sgRNA) designed to target a conserved region of exon 1 among the three *TaSPL8* homeologs. The protospacer-adjacent motif (PAM) sequence is highlighted in red. D, The genotypes of three mutant lines were identified by sequencing. The symbols "+" and "−" indicate the insertion or deletion caused by CRISPR/Cas9-induced mutations, respectively. Numbers indicate the length of the insertion or deletion. E, Flag leaf phenotypes of mutant *Taspl8-2A/2B/2d*, *cpa* and LC10. Bars = 1 cm. F, Flag leaf angle and lamina joint length of *Taspl8-2A/2B/2d*, *cpa* and LC10 plants. The double asterisk represents significant differences determined by two-tailed Student's *t* test at $P < 0.01$. Error bars = SD ($n = 10$).

CRISPR/Cas9 system. Due to the nucleotide similarity among *TaSPL8-2A*, *TaSPL8-2B*, and *TaSPL8-2D*, sgRNA specifically targeting to *TaSPL8-2D* cannot be designed. Thus, a sgRNA targeting a conserved region within the first exon of the *TaSPL8-2A*, *TaSPL8-2B*, and *TaSPL8-2D* was designed and the CRISPR/Cas9 vector *pBUE411::sgRNA* was introduced into LC10 (Fig. 3C). A total of 10 independent transgenic T_0 plants (KO lines) were obtained and three lines with all three homeologous genes mutated simultaneously were selected for further analysis. Frameshift mutations in all three subgenomes were also detected in the T1 offspring (Fig. 3D). The KO-2-1 line was backcrossed to LC10 to generate the *TaSPL8-2A/2B/2d* single mutant, which showed a smaller lamina joint and flag leaf angle similar to the *cpa* mutant, compared with LC10 (Fig. 3, E and F). These results indicated that the loss of *TaSPL8-2D* is responsible for the *cpa* mutant phenotype.

Three Homeologous Genes of *TaSPL8* Differentially Contribute to Lamina Joint Growth

One extraordinary feature of polyploid evolution is genomic asymmetry, which is the predominant control of a variety of morphological, physiological, and molecular traits by one subgenome over the others, which prompted us to determine the functional divergence of *TaSPL8* from 2A, 2B, and 2D subgenomes (Wang et al., 2016). We firstly compared the sequence similarity of open reading frames (ORFs) and protein sequences of the three *TaSPL8* homeologous genes, and they showed 97.2% and 97.5% similarities for nucleotide and amino acid sequences, respectively. Primer combinations located in the coding sequence region specific for each homeolog were designed and verified using the Chinese Spring null-tetrasomic lines of chromosome group 2. We found that the PCR fragments could not be amplified when the corresponding chromosome was deleted (Fig. 4A). Using these primers, the transcript level of *TaSPL8-2D* was observed to be higher than that of *TaSPL8-2A* and *TaSPL8-2B* in the lamina joint (Fig. 4B).

Possible divergence among these homeologs in their contribution to the observed phenotype was investigated by generating single, double, and triple mutants for each homeolog. As mentioned above (Fig. 3D), we firstly obtained the triple mutant *TaSPL8-2a/2b/2d* by gene editing. The KO-2-1, KO-3-1, and KO-7-1 mutants with three *TaSPL8* homeologs knocked out simultaneously showed erect leaves at both vegetative and reproductive stages (Fig. 4, C and D), with a notable decrease in flag leaf angle compared to the wild-type LC10 (Fig. 4D). Additionally, the lamina joint was severely affected and the boundary between the blade and sheath was absent in these KO lines (Fig. 4, E and F). Similar phenotypes were also observed for the KO lines in CB037 and Bobwhite recipients (Supplemental Fig. S3). The triple mutant KO-2-1 was crossed to wild-type LC10 to generate single and double mutants. Compared to LC10, the *TaSPL8-2a/2B/2D* single mutant did not show differences in lamina joint length, while the *TaSPL8-2A/2b/2D* and *TaSPL8-2A/2B/2d* single mutants had a shorter lamina joint, with the major effect detected in *TaSPL8-2A/2B/2d* (Fig. 4, G and H). Accordingly, the double mutant *TaSPL8-2a/2B/2d* had a smaller lamina joint length compared with the *TaSPL8-2a/2b/2D* double mutant, indicating that the *TaSPL8-2D* homeolog provides the major contribution for the lamina joint length phenotype (Fig. 4, G and H). Observations from double mutants also corroborated the information from single mutants that *TaSPL8-2B* affects lamina joint length to a greater extent than *TaSPL8-2A* (Fig. 4, G and H). These results indicated that the homeologous gene from the D subgenome contributed to lamina joint length to a greater extent than those from the A and B subgenomes.

To evaluate the potential of manipulating *TaSPL8* for optimizing wheat leaf architecture and improving grain yield, we compared the yield-related traits of the *TaSPL8* mutant KO-2-1 and the wild-type LC10 in different planting populations of 300, 450, 600, and 750 seeds/m^2 in two different locations (Beijing and Yangling). Spike numbers per plant for the KO-2-1 line were higher compared to LC10, especially at dense planting populations (450, 600, and 750 seeds/m^2; Fig. 4I), which could contribute to higher grain yield. Other traits, including plant height, spike length, grain number per spike, grain weight, heading date (flowering time), and the grain-filling period (time to maturity) did not differ between the KO-2-1 line and LC10 (Supplemental Table S1).

Natural Variation of *TaSPL8-2D*

To determine the variation of *TaSPL8-2D* in a natural wheat population, 192 wheat cultivars were screened for nucleotide polymorphisms. No single nucleotide polymorphism was identified in the coding and promoter region, suggesting that the *TaSPL8-2D* sequence is conserved because of its pivotal role in controlling lamina joint development. The *TaSPL8* expression level and lamina joint length was also assessed in 78 wheat cultivars, including 29 cultivars with larger lamina joints (1.5–2.6 cm) and 49 cultivars with smaller lamina joints (0.8–1.5 cm; Supplemental Table S2). The results indicated that the *TaSPL8* mRNA level in the lamina joint is higher in cultivars with larger lamina joints compared to those with smaller lamina joints (Fig. 4J). These results further corroborated the role of *TaSPL8* in lamina joint development.

TaSPL8 Regulates Lamina Joint Development Through the Auxin and BR Pathways

To understand the mechanisms behind *TaSPL8*-mediated lamina joint regulation, we performed a transcriptome analysis using RNA-seq in the lamina joint of main tiller from *TaSPL8-2a/2b/2d* (two independent

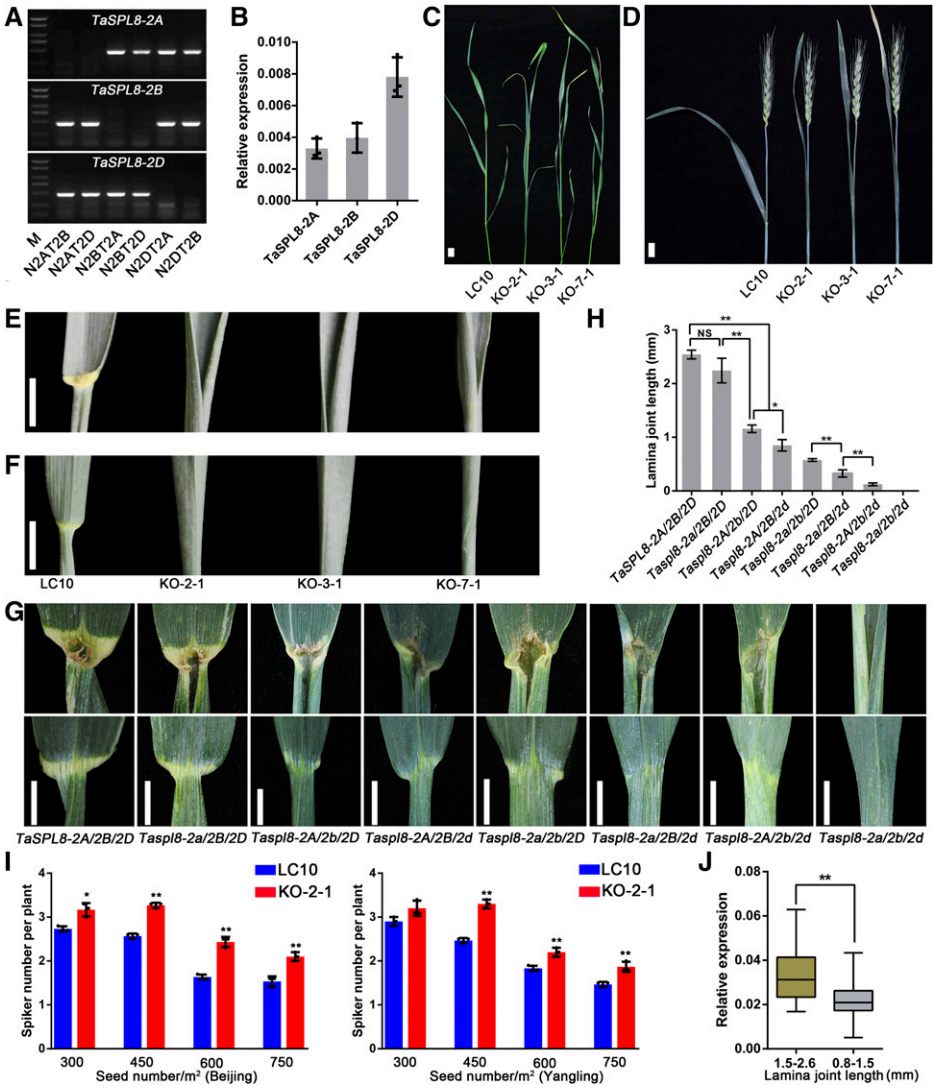

Figure 4. Three homeologous genes of *TaSPL8* differentially contribute to lamina joint growth. A, The specificity of primers for three *TaSPL8* homeologous genes were verified by amplifying the genomic DNA of the wheat cultivar Chinese Spring nullitetrasomic lines of chromosome group 2, where N2DT2B represents nullisomic2D-tetrasomic2B, for example. B, Relative abundance of three homeologous genes, *TaSPL8-2A*, *TaSPL8-2B*, and *TaSPL8-2D*, in the lamina joint. DNA of the Chinese Spring cultivar was used to analyze the amplification efficiency of the three pairs of primers. The RT-qPCR data were normalized to wheat *TaACTIN* and each bar in the graph corresponds to the mean value of three data points, shown by dots. C and D, Leaf phenotype of LC10 and mutant lines at heading (C) and flowering stages (D). Bars = 2 cm. E and F, Adaxial (E) and abaxial side (F) phenotypes of the lamina joint region of LC10 and mutant lines. Bars = 2 cm. G, Lamina joint phenotype of *TaSPL8* single, double, and triple homeologous mutant plants. Bars = 1 cm. H, The lamina joint length of *TaSPL8* single, double, and triple homeologous mutants. The values shown are averages from three plants and the SD is indicated. NS, nonsignificant. Single and double asterisks represent statistically significant differences determined by the two-tailed Student's *t* test at $*P < 0.05$ and $**P < 0.01$, respectively. I, Spike number per plant in LC10 and mutant lines in different planting densities (300, 450, 600, and 750 seeds/m^2) in Beijing and Yangling. The values shown are averages from three replicates and the SD is reported. Single and double asterisks represent statistically significant differences determined by the two-tailed Student's *t* test at $*P < 0.05$ and $**P < 0.01$, respectively. J, Comparison of *TaSPL8* expression levels between the wheat cultivars with larger (1.5–2.6 mm; $n = 29$) and smaller (0.8–1.5 mm; $n = 49$) lamina joints. The level of *TaSPL8* mRNA was normalized to wheat *ACTIN*. Lines in the box plots indicate the median. The 10th/90th percentiles of outliers are shown. The double asterisk represents statistically significant differences as determined by Student's *t* test at $**P < 0.05$.

KO lines: KO-2-1 and KO-7-1) and *TaSPL8-2A/2B/2d* (single KO line) mutants, as well as of LC10 wild-type plants at the heading stage. For each sample, three biological replicates were employed. The *TaSPL8-2A/2B/2d* mutant was included in the experiments because the triple *TaSPL8-2a/2b/2d* mutant lacks the lamina

joint and the cell type between the sheath and blade are completely different with respect to LC10, while the single mutant exhibits a phenotype more similar to the wild type, but with a noticeable decrease in lamina joint length. The results indicated that 5,980 genes are downregulated and 2,986 genes are upregulated in the *TaSPL8-2a/2b/2d* mutants compared to LC10 (Fig. 5A; Supplemental Tables S3 and S4). Furthermore, a comparison between the *TaSPL8-2A/2B/2d* single mutant and the wild type indicated that 1,841 genes are downregulated and 1,509 are upregulated (P values < 0.05, $|\text{Fold Change}| > 2$). Among the differentially expressed genes (DEGs), 408 and 1,310 genes are upregulated and downregulated, respectively, in both the triple and single *TaSPL8-2D* mutant (Fig. 5A).

GO functional annotation of the DEGs shared between the triple and single *TaSPL8* mutants revealed statistically significant enrichment in downregulated genes for pathways related to response to auxin, metabolic process for carbohydrate, cellular glucan, xyloglucan, biosynthetic process for fatty acid, cellulose, and cell wall (Fig. 5B). Among the upregulated genes, we found an enrichment in pathways associated with protein phosphorylation and photosynthesis (Fig. 5B). For cell component ontology, downregulated genes were enriched in the extracellular region and apoplast and cell wall, whereas upregulated genes were enriched in PSI and PSII (Fig. 5C). These observations suggest *TaSPL8* involvement in cell wall development through the auxin pathway.

Among the DEGs in the single and triple *TaSPL8* mutants, we found 188 downregulated genes related to auxin signaling, including the auxin-responsive Aux/IAA gene family (IAAs), ARFs, auxin efflux carrier components PIN-FORMED (PIN), small auxin-upregulated RNA, and GH3 family (Supplemental Fig. S4; Supplemental Tables S3 and S4). Measurement of the IAA content in the lamina joint region (tissue between the blade and sheath) of LC10 and the *TaSPL8-2a/2b/2d* mutant indicated that the IAA content was similar between the mutant and the wild type (Fig. 5D), indicating that *TaSPL8* does not affect IAA biogenesis but may act through auxin response signaling.

Another interesting category of DEGs that were downregulated in the single and triple *TaSPL8* mutants include genes involved in cell division, cell elongation, and the cytoskeleton (Supplemental Fig. S4; Supplemental Tables S3 and S4). Downregulation of these genes may lead to failure of cell elongation and result in the lamina joint defects observed in the mutants. These effect can be envisaged especially for the 128 genes encoding glycosyl hydrolase (which function in primary cell wall structure; López-Bucio et al., 2002), the 48 genes for expansins (which regulate cell wall extension; Cosgrove, 2015), and seven genes for pectinacetylesterase (which function in cell wall extensibility by enhancing aggregation processes between galacturonan chains inside the apoplasm; Sénéchal et al., 2014).

Finally, among the downregulated DEGs, we found three genes with high similarity to rice *BRD1/OsDWARF/OsBR6ox*, *BRD2*, and *Cytochrome P450 90D2* (*D2/CYP90D2*), which are implicated in BR biosynthesis processes (Supplemental Fig. S4; Supplemental Tables S3 and S4). Moreover, 14 genes encoding *BRASSINOSTEROID INSENSITIVE1*-associated proteins

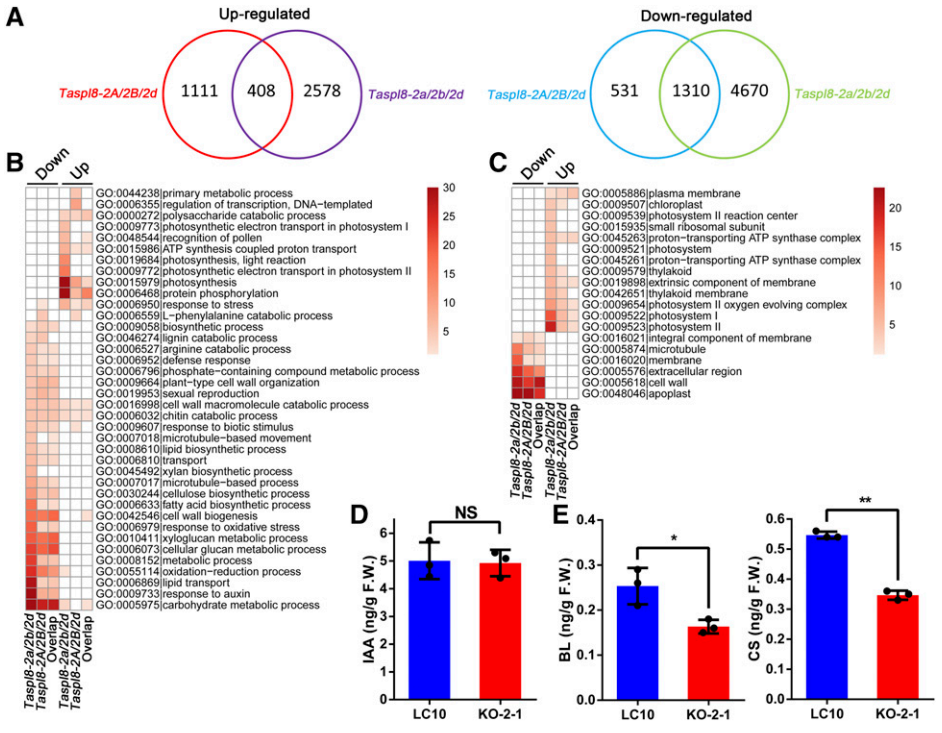

Figure 5. Gene Ontology (GO) term enrichment analysis and IAA/BR level measurement in *TaSPL8* mutants and wild-type plants. A, Venn diagram analysis of DEGs in *TaSPL8-2A/2B/2d* and *TaSPL8-2a/2b/2d* mutants compared to the wild type (LC10). B, GO terms for biological processes exhibiting statistically significant enrichment in DEGs (only DEGs in common for both single and triple *TaSPL8* mutants were considered). C, GO terms for cell components exhibiting statistically significant enrichment in DEGs. D and E, IAA, Brassinolide (BL), and Castasterone (CS) levels were measured in the lamina joint tissue of LC10 and KO-2-1 (*TaSPL8-2a/2b/2d*) plants. Single and double asterisks represent statistically significant differences determined by the two-tailed Student's t test at $^*P < 0.05$ and $^{**}P < 0.01$, respectively. Error bars = SD ($n = 3$). NS, not significant.

and *BRASSINAZOLE-RESISTANT1* homolog proteins, which are responsive to the BR signaling pathway, were also among the downregulated DEGs (Supplemental Fig. S4; Supplemental Tables S3 and S4). In agreement with these observations, we found that the brassinolide and castasterone content in the *TaSPL8-2a/2b/2d* mutant is reduced in comparison with LC10 (Fig. 5E), indicating that *TaSPL8* affects BR biosynthesis and signaling pathways. Altogether, our findings indicate that *TaSPL8* might regulate lamina joint development through BR and auxin pathways, which are essential for both cell elongation and cell proliferation.

TaSPL8 Acts as a Transcriptional Activator of *AUXIN RESPONSE FACTOR* and *TaD2*

Because maize LG1 is expressed in ligule and activates PIN1a expression as a transcription activator (Johnston et al., 2014), we screened the downregulated DEGs identified in our transcriptome analysis for the presence of the 16-nt sequence containing a GTAC core motif (Motif ID: MA0578.1) in their putative promoters, which was previously identified as the cis-element of AtSPL8 targets in Arabidopsis (*Arabidopsis thaliana*; Kropat et al., 2005). Among the 5,980 downregulated genes in the *TaSPL8-2a/2b/2d* mutant, 1,687 have this motif in their putative promoter sequence, as tested using the software FIMO (http://meme-suite.org/tools/fimo). The ability of TaSPL8 to bind to the sequence containing the GTAC core motif was assessed using electrophoretic mobility shift assays (EMSAs). To this end, nine probes were synthesized from the promoters of three auxin-responsive genes and four cell expansin genes. The results indicated that TaSPL8 can bind to these probes (Supplemental Fig. S5).

Among the DEGs downregulated in the *TaSPL8* mutant, one gene *TraesCS5B01G039800* (*TaARF6*) is the putative ortholog of Arabidopsis *AtARF6* (Supplemental Fig. S6). ARFs are key players in mediating auxin-induced gene activation (Lau et al., 2008). In addition, we found that *TraesCS5B01G039800* is upregulated in wild-type LC10 plants after exogenous auxin treatment, although it does not respond to auxin in the KO-2-1 (*TaSPL8-2a/2b/2d*) mutant (Fig. 6A). Therefore, we investigated whether *TaSPL8* acts in auxin signaling by directly activating the expression of *ARF* genes. Similarly, we also tested whether *TaSPL8* activates the expression of genes involved in BR biosynthesis because *TraesCS3A01G103800* (*TaD2*), the putative ortholog of rice *D2*, is strongly downregulated in *TaSPL8* mutants. Rice *D2* encodes a cytochrome P450, which catalyzes the steps from 6-deoxoteasterone to 3-dehydro-6-deoxoteasterone and from teasterone to 3-dehydroteasterone in the late BR biosynthesis pathway. The results of our EMSAs revealed that binding of a TaSPL8 recombinant protein to the putative promoters of *TaARF6* and *TaD2* occurs in vitro (Fig. 6, B and C).

To determine if the direct binding also takes place in vivo, we first generated a overexpression transgenic wheat line (OE lines) in which *TaSPL8* was fused to Myc tag and driven by promoter of maize *UBIQUTIN1* (*ProUbi*::*TaSPL8-9MYC*) and then performed chromatin immunoprecipitation (ChIP) assays with a Myc-specific antibody. We achieved three independent transgenic lines (OE-5, OE-10, and OE-12) with high levels of *TaSPL8* mRNA and TaSPL8-9Myc protein (Fig. 6D). Compared to the wild type of reference (CB037), the OE lines were smaller and displayed fewer tiller numbers at the seedling stage, and decreased spike length and grain size (Supplemental Fig. S7). ChIP followed by qPCR was performed from the lamina joint tissue of the OE lines and wild-type CB037. The results indicated that TaSPL8-MYC enrichment of the GTAC core motif of *TaARF6* and *TaD2* in OE lines is significantly higher than that in wild-type CB037 and its enrichment in another region (outside GTAC core motif) is very low, suggesting that TaSPL8 specifically binds to the promoter region of *TaARF6* and *TaD2* with the GTAC core motif (Fig. 6E). The effect of TaSPL8 binding to the *TaARF6* and *TaD2* promoter was investigated using a transient expression assay. Specifically, a plasmid containing the promoter of *TaARF6* (*pTaARF6*::*LUC*) or the *TaD2* promoter (*pTaD2*::*LUC*) driving the expression of the luciferase (LUC) reporter gene was cotransformed in tobacco (*Nicotiana tabacum*) leaves with the effector plasmid (*35S*::*TaSPL8*) expressing TaSPL8. The results indicated that TaSPL8 can activate the expression of the reporter for both promoters (Fig. 6F). Overall, these findings indicate that TaSPL8 directly binds to the promoter of *TaARF6* and *TaD2* in the region containing the GTAC motif, which is also associated with their transcriptional activation. Therefore, we can envisage that one of the mechanisms underlying *TaSPL8*-mediated regulation of lamina joint development involves the direct activation of key genes of auxin signaling and BR biogenesis.

DISCUSSION

TaSPL8 and Its Homolog *LG1* in Maize and Rice Could Be a Robust Target for Plant Architecture Improvement in Grass

Erect leaves improve light interception and biomass production under field conditions, resulting in increased grain yield in grass crops (Sakamoto et al., 2006). The erect-leaf phenotype of a rice BR-deficient mutant, *osdwarf4-1*, is associated with enhanced grain yields under dense planting populations, even without extra fertilizer (Sakamoto et al., 2006). Therefore, it can be assumed that a compact plant architecture mediated by erect leaves is also an important goal for wheat breeding, but no potential target genes for breeding programs have been identified to date in wheat. This study provides information about the role and mechanisms of *TaSPL8*, which encodes an SPL-like transcription factor, in controlling leaf angle by regulating lamina joint development. Lamina joint formation is

impaired in *TaSPL8* KO mutants, resulting in erect leaves and a more compact architecture. Our findings suggest that *TaSPL8* is an important regulator of compact architecture in wheat, and therefore, could be used as a target to achieve elite wheat cultivars with erect leaves through genetic engineering and molecular breeding.

TaSPL8 plays a similar function in lamina joint development as *LG1* in maize and rice. The mutation of *LG1* in maize and rice also resulted in an erect leaf phenotype with a complete loss of the auricle and ligule (Moreno et al., 1997; Lee et al., 2007). Although the contribution of maize and rice *LG1* to potential yield in high density planting is still unknown, we speculated that this gene might be a robust target for compact plant architecture in grass, considering the highly conserved function in lamina joint development. However, we have to consider the functional variation among *LG1* genes of maize, rice, and wheat. Beside affecting ligule development, *OsLG1* regulates panicle closure or spreading by controlling cell proliferation at the panicle pulvinus (Ishii et al., 2013; Zhu et al., 2013). *ZmLG1* also controls the branch angle of the tassel and its KO mutants result in a more compact tassel than their wild-type counterparts (Bai et al., 2012). Different from *OsLG1* and *ZmLG1*, *TaSPL8* does not affect the spike

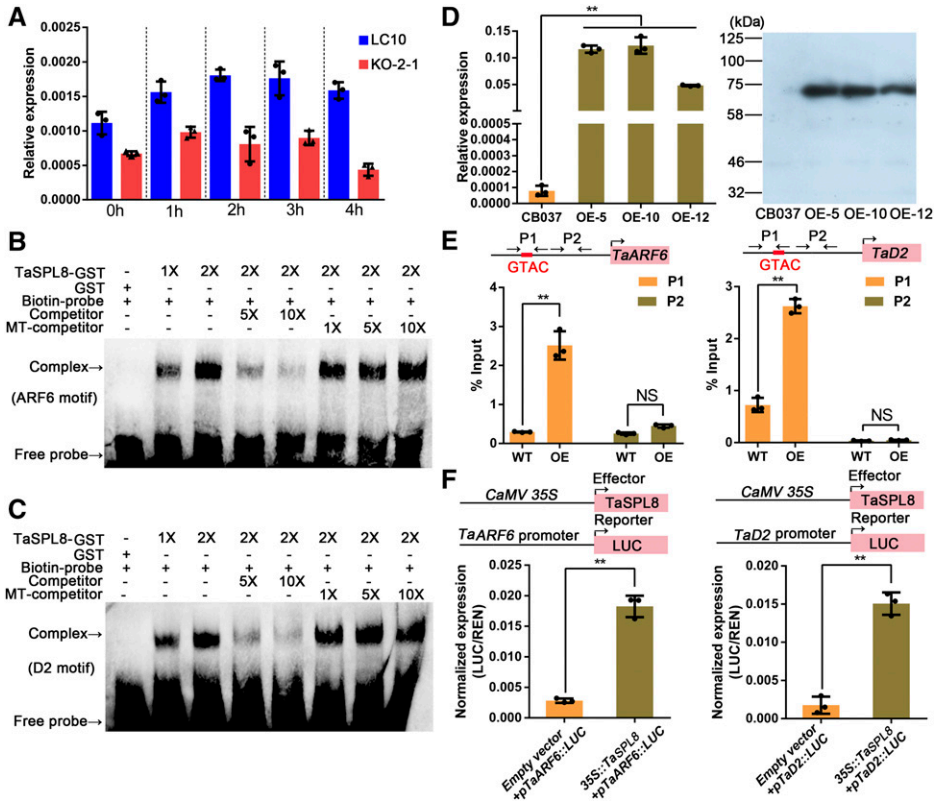

Figure 6. TaSPL8 binds and activates *TaARF6* and *TaD2*. A, *TaARF* expression analysis after auxin treatment (10^{-4} mol/L) in the wild-type LC10 plant and a *TaSPL8* mutant (KO-2-1). Each bar in the graph corresponds to the mean value of three data points, shown by dots. B and C, EMSAs to assess the TaSPL8 binding to the promoter region of *TaARF6* (B) and *TaD2* (C) containing the GTAC motif. The symbols "+" and "−" indicate the presence and absence, respectively, of corresponding probes, proteins, or competitors. The terms "1X" and "2X" indicate amounts of protein in the reaction. The terms "5X" and "10X" indicate 5- and 10-fold molar excess, respectively, of competitor or mutated competitor (MT) probes relative to biotin-labeled probes. D, Generation of wheat transgenic lines overexpressing TaSPL8-Myc chimeric protein (overexpressing [OE] lines) in the CB037 genetic background. The level of *TaSPL8* transcripts (left) and TaSPL8-Myc protein (right) were measured. RT-qPCR data were normalized to wheat *TaACTIN* and each bar in the graph corresponds to the mean value of three data points, shown by dots. Double asterisks represent statistically significant differences determined by the two-tailed Student's *t* test at $^{**}P < 0.01$. E, ChIP assays to detect TaSPL8 binding of *TaARF6* and *TaD2* in vivo. Arrows indicate the position (P1 and P2) of primer combinations used in qPCR after ChIP assays. "P1" indicates the region where GTAC is located and "P2" indicates the region without GTAC with more than 400-bp distance from P1. Each bar in the graph corresponds to the mean value of three data points, shown by dots. Double asterisks represent statistically significant differences determined by the two-tailed Student's *t* test at $^{**}P < 0.01$. WT, wild type. F, Transactivation assays with tobacco leaves infiltrated with different combinations of effector and reporter constructs. Individual values (black dots) and means (bars) of three independent biological replicates are shown. The double asterisks represent significant differences determined by the two-tailed Student's *t* test at $^{**}P < 0.01$. LUC/REN (Renilla luciferase) indicates the ratio of the firefly luciferase activity and the renilla reniformis activity.

structure, while directly or indirectly leading to the alteration of spike numbers. *TaSPL8* mutants show increased spike numbers especially under dense planting condition. This phenotype may be due to erect leaves that allow greater penetration of light to the lower leaves, thereby improving canopy photosynthesis, which, in turn, improves the formation of tillers or the ability to generate a spike. A similar phenotype was observed in the *osdwarf4-1* rice mutant with erect leaves due to BR deficiency (Sakamoto et al., 2006). Alternatively, *TaSPL8* may directly regulate tiller and spike formation. *TaSPL8* is highly expressed both in the lamina joint and young spikes and overexpressing plants show a clear reduction in tiller number and spike size. However, an overexpression transgenic line driven by the *Ubi* promoter actually shows an ectopic effect from the early growth stage. Ubiquitous overexpression may affect the natural function of a gene/protein, for example by altering transcription factor binding specificity when binding is sensitive to doses, or by altering the stoichiometric composition of a multiprotein complex, thus affecting its possible activity and specificity. Therefore, ubiquitous overexpression mutants are not the best for judging a gene's function, because pleiotropic and "artificial" effects are more likely to be observed. The specific upregulation of *TaSPL8* in spikes or tillers will help us to understand its biological function.

A wild species can be changed to a new form to meet human needs through crop domestication. *OsLG1* has experienced substantial artificial selection during rice domestication (Ishii et al., 2013; Zhu et al., 2013). The selection of a single-nucleotide polymorphism residing in the cis-regulatory region of the *OsLG1* gene was responsible for the transition from a spread panicle typical of ancestral wild rice to the compact panicle of present cultivars during rice domestication (Zhu et al., 2013). This selection led to the reduced expression of *OsLG1* specifically at the panicle pulvinus while maintaining normal levels during ligule formation (Zhu et al., 2013). In wheat, we found that the level of *TaSPL8* mRNA in the lamina joint is higher in modern cultivars with larger lamina joints ($n = 49$) compared to those with smaller lamina joints ($n = 29$; Fig. 4J), indicating that *TaSPL8* is also selected for leaf angle during wheat breeding. However, we did not find sequence variation in the cis-regulatory region of *TaSPL8* among these cultivars. Hence, genetic variation in possible distal regulatory elements or epigenetic variation in the *TaSPL8* promoter may account for the observed difference in the transcript level.

TaSPL8-2D Is a Major Contributor to Erect Leaf in Wheat

Common wheat is an allohexaploid (BBAADD) derived from a hybridization between a cultivated form of allotetraploid wheat *Triticum turgidum* (BBAA) and diploid goat grass *A. tauschii* (DD). *T. turgidum* originates from the hybridization and polyploidization of the diploid species *T. urartu* (AA) and *A. speltoides* (SS genomes, most probably the donor of the B genome). The combination and interaction of subgenomes in the allohexaploid give rise to phenotypic variation during wheat evolutionary history. The evolution of duplicated gene loci in allopolyploid plants contribute either to a favorable effect of extra gene dosage or to built-up asymmetric expression divergence: only one genome is active, whereas the homoeoalleles on the other genome(s) are either eliminated or partially or completely suppressed by genetic or epigenetic means (Feldman et al., 2012). However, there is no evidence showing how asymmetric expression divergence affects the trait. We found that the expression level of homoeoallele *TaSPL8-2D* was higher in the lamina joint compared to the expression level of *TaSPL8-2A* and *TaSPL8-2B*. Observations from single, double, and triple mutants also corroborated the information that the *TaSPL8-2D* homeolog provides the major contribution for the lamina joint length phenotype and *TaSPL8-2B* affects lamina joint length to a greater extent than *TaSPL8-2A*. These data expand our knowledge about genome asymmetry during allopolyploid wheat evolution and suggest a possible mechanism and evolutionary advantage of this divergence, but addressing this requires further work.

The Utilization of *TaSPL8* for Compact Plant Architecture in Wheat Breeding

Simultaneous mutations of all three *TaSPL8* homeologs lead to the absence of the lamina joint, sometimes resulting in flag leaves wrapping around the spikes, which blocks spike extension. Thus, potential routes for *TaSPL8* utilization in wheat breeding include: (1) using a single mutation of *TaCAP-2D* or *TaCAP-2B* to obtain a shorter lamina joint without affecting spike extension; and (2) using alleles associated with lower expression of *TaSPL8* and shorter lamina joints, which could be used in marker-assisted selection to fine-tune lamina joint length and leaf angle.

TaSPL8 Modulates Leaf Angle through Auxin and BR Signaling

LG1 orthologs in maize, rice, and wheat function as key regulators of lamina joint development. ZmLG1 was found to function downstream of maize TEOSINTE BRANCHED 1/CYCLOIDEA/PCF transcription factor (Lewis et al., 2014) and to regulate a series of downstream genes such as *PIN1* and gene encoding for a homeobox-transcription factor 48, which were identified by comparing transcript accumulation between an *lg1* mutant and wild type in the preligule region (Johnston et al., 2014). Our study provides evidence that TaSPL8 affects lamina joint development by directly activating the expression of genes involved in auxin and BR pathways. Previous findings indicated that these hormones and various transcription factors

contribute to cell division and elongation at the lamina joint region (Sakamoto et al., 2006; Bian et al., 2012; Zhao et al., 2013). Here, we have identified the mechanistic link between one transcription factor and the auxin and BR pathways, which are involved in lamina joint development and leaf architecture. Specifically, we found that TaSPL8 directly binds and activates *TaARF6*, which is involved in the auxin signaling pathway, and *TaD2*, which regulates BR biosynthesis (Fig. 7). Auxin is essential for cell elongation in nearly all developmental processes. The two Arabidopsis *TaARF6* orthologs, *ARF6* and *ARF8*, are required for cell elongation in the inflorescence stem, stamen filament, stigmatic papillae, and hypocotyls, and in anther dehiscence (Nagpal et al., 2005; Oh et al., 2014; Liu et al., 2018a). TaARF6 may similarly act as a regulator of cell elongation in the lamina joint. This scenario is supported by findings that other members of the *ARF* gene family regulate leaf angle. *OsARF19*-overexpressing rice lines show multiple phenotypes, including increased leaf angles (Zhang et al., 2015), and an *OsARF11* loss-of-function line exhibits a reduced angle of the flag leaves (Sakamoto et al., 2013). Similarly, rice mutants with impaired expression of *ebisu dwarf*, the ortholog of wheat *TaD2*, are deficient in BR biogenesis and have erect leaves (Hong et al., 2003). This strongly supports our findings that another form of *TaSPL8*-mediated regulation of lamina joint development occurs through transcriptional activation of *TaD2* and the subsequent increase in BR biosynthesis. Although rice BR-deficient mutants are usually dwarfed with short internodes, *TaSPL8* mutants do not exhibit other phenotypic alterations except for lamina joint development. We speculate that high expression of *TaSPL8* in lamina joint tissue specifically regulates BR biogenesis in this region. Our results indicate that *TaSPL8* also affects the expression of genes involved in cell elongation and expansion. For example, we found that 48 genes for expansins are downregulated in the *TaSPL8-2a/2b/2d* mutant, and TaSPL8 can bind to the GTAC motif of the promoters of four cell expansin genes in vitro (Supplemental Fig. S5). This suggests that TaSPL8 regulates lamina joint development by directly targeting expansin genes. An alternative and not mutually exclusive possibility is that *TaSPL8* regulates expansin genes through auxin signaling, because cell elongation genes are also responsive to auxin (Pacheco-Villalobos et al., 2016).

In conclusion, this study reveals the mechanisms that link one member of the SPL transcription factor family with hormones in regulating lamina joint development, in that *TaSPL8* acts upstream of genes involved in the regulation of lamina joint cell elongation, such as *TaARF6* and *TaD2*, which mediate the auxin signaling pathway and BR biosynthesis, respectively. In addition, our results identify additional genes that may function in lamina joint development (e.g. *expansin*). These findings will be useful for programs aimed at manipulating wheat architecture for improved grain yield.

MATERIALS AND METHODS

Plant Materials

Names and geographical origins of all wheat (*Triticum aestivum*) cultivars used in this study are listed in Supplemental Table S2. Plant materials used for visible phenotypic, microscopic, and molecular analyses were grown in a greenhouse at a relative humidity of 75% and 26°C/20°C day/night temperatures, with a light intensity of 3,000 lx (Master GreenPower CG T 400W E40; Philips). Wheat cultivars used for seed reproduction and phenotypic analysis were grown in the experimental field of China Agricultural University in Beijing (39°57′N, 116°17′E), Yangling in the Shaanxi province (34°16′N, 108°04′E). Lamina joints for gene expression analysis were harvested at the heading stage. For each sample, the lamina joint from three different planting pots was harvested, representing three biological replicates. All samples were immediately frozen in liquid nitrogen and stored at −80°C. The natural wheat population consisted of 192 wheat cultivars including Chinese landraces (111), Chinese modern cultivars (42), and foreign cultivars from other countries in Europe, Asia, America, and Australia (39).

Phenotypic Analysis

The length of the lamina joint and auricle were measured as the widest section between the leaf blade and the sheath with a Vernier caliper. Flag leaf angle was

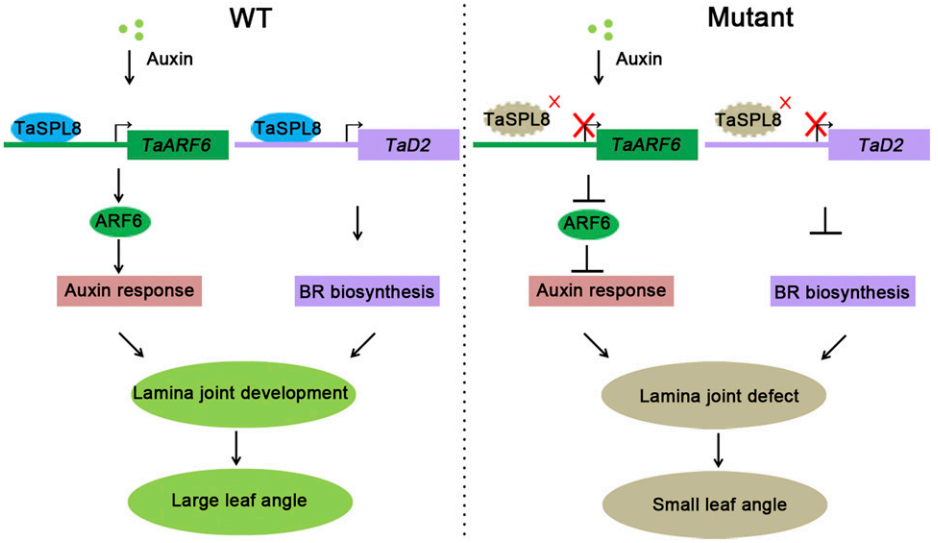

Figure 7. Molecular model for the regulation of wheat lamina joint development by *TaSPL8*. TaSPL8 directly binds to the *TaARF6* and *TaD2* promoters to activate their expression. *TaARF6* mediates the auxin signaling pathway, whereas *TaD2* is involved in BR biogenesis. Both hormones are well known for regulating cell elongation, lamina joint development, and leaf angle. WT, wild type.

measured using a protractor between the stem under the spike and the flag leaf midrib. Plant height and the length of the main spike were measured before harvesting, and 10 main spikes were bagged at the same time to measure fertile grain number per spike and grain weight per 1,000 grains. Spike number per plant was calculated as the average value of 10 plants. A randomized complete block design with three replicates was employed for phenotyping in open field experiments.

Mapping of *TaSPL8*

Fine mapping was performed with an F2 and F2-derived F_3 population from a cross between *cpa* and LC10. Primers used for fine mapping were designed based on the sequence of Chinese Spring (IWGSCv1; http://www.wheatgenome.org/) and *Aegilops tauschii* (Luo et al., 2017) and listed in Supplemental Table S5. NILs in the cpa genetic background containing the LC10 allele (NIL^{LC10}) and NILs in the LC10 genetic background containing the *cpa* allele (NIL^{cpa}) were generated through backcrossing LC10 × *cpa* F1 plants to LC10 and the *cpa* mutant for BC_3, respectively. The introgression fragment between markers *2D-173* and *LMC-3* was screened at each generation. The BC_3F_1 plant was self-crossed to generate NIL^{LC10} and NIL^{cpa}, respectively.

Plasmid Construction and Transformation

For genome editing via CRISPR/Cas9, a sgRNA was designed in the first exon sequence of *TaSPL8* using the E-CRISP Design Web site (http://www.e-crisp.org/E-CRISP/designcrispr.html). Two reverse complementary sgRNA sequences with the *Bsa*I cohesive ends were synthesized. Double-stranded oligonucleotides were annealed by cooling from 100°C to room temperature, followed by insertion into the expression cassette of the pBUE411 vector (Xing et al., 2014). Plasmids were transformed into three wheat cultivars (CB037, LC10, and Bobwhite) using *Agrobacterium*-mediated (strain EHA105) transformation (Ishida et al., 2015). For *TaSPL8* overexpression, the ORF of *TaSPL8-2D* from CB037 and the nine repeated Myc domain sequences were amplified and linked by PCR, then the *TaSPL8-9Myc* fragment was inserted into the pMWB122 vector (Wang et al., 2017) using *Sma*I and *Spe*I cloning sites to achieve the *ProUbi*::*TaSPL8-9Myc* construct. Plasmids were transformed into the wheat cultivar CB037 using *Agrobacterium*-mediated (strain EHA105) transformation (Ishida et al., 2015).

RT-qPCR Analysis

Total RNA was extracted from different tissues using TRIzol reagent (Takara) according to the manufacturer's instructions and cDNA was synthesized by a reverse transcription kit (Vazyme Biotech). Wheat *TaACTIN* (*TraesCS5B01G124100*) was used as an internal control. For RT-qPCR, the reaction mixture was composed of the cDNA first-strand template, primers, and SYBR Green Mix (Takara) to a final volume of 10 μL. Reactions were performed using the CFX96 real-time system (Bio-Rad). For technical replicates, the RT-qPCR for each sample was replicated three times. Three biological replicates were performed (one replication is shown). The average values of $2^{-\Delta CT}$ were used to determine the differences in gene expression (https://assets.thermofisher.com/TFS-Assets/LSG/manuals/cms_040980.pdf).

ChIP-qPCR Assay

Wheat leaves were cross-linked in fixative buffer (1% [v/v] volume/volume formaldehyde) by vacuum infiltration. Cross-linking reactions were stopped by adding Gly at a final concentration of 0.17 M. Chromatin extracts were sonicated and precleared with Dynabeads protein A agarose (Merck Millipore) for 1 h. For immunoprecipitation, anti-Myc antibody (cat. no. ab9132; Abcam) was added and samples were incubated at 4°C overnight. The chromatin-antibody complex was recovered with Dynabeads protein A+G and beads were washed sequentially with low salt wash buffer, high salt wash buffer, LiCl wash buffer, and Tris-EDTA buffer for 5 min each (Yang et al., 2016). The protein/DNA complex was eluted with elution buffer (1% [w/v] weight/volume SDS and 0.1 M of $NaHCO_3$). Cross-linking was reversed by adding NaCl at a final concentration of 200 mM, followed by incubation for 5 h at 65°C. Proteins in the resulting complex were removed by proteinase K at 45°C for 1 h. DNA was precipitated in the presence of three volumes of ethanol and one-tenth volume of 3-M sodium acetate at pH 5.2. Precipitated DNA was dissolved in 30 μL of 10-mM Tris-HCl at pH 7.5, and treated with RNase (DNase-free). Two independent ChIP assays were performed for each sample. qPCR was carried out using the CFX96 real-time system (Bio-Rad). ChIP values were normalized to their respective DNA input values, and the fold changes in concentration were calculated based on the relative enrichment in the overexpression lines compared with wild-type immunoprecipitates. Primer sequences used in the qPCR analysis are listed in Supplemental Table S5.

Transient Expression in Tobacco Leaves

Dual luciferase reporter assays were performed as described in Guan et al. (2014). A fragment corresponding to 1,800 bp upstream of the transcription start site of *TaARF6* was PCR-amplified from LC10 genomic DNA and cloned into the pGreenII 0800-LUC vector (Hellens et al., 2005), generating the reporter pGreenII *pTaARF*::*LUC* and *pTaD2*::*LUC* plasmids. The ORF of *TaSPL8* was cloned into the pUC18-35S vector generating the effector *35S*::*TaSPL8* plasmid. Young leaves of 4-week–old tobacco (*Nicotiana tabacum*) plants were coinfiltrated with *Agrobacterium* (strain GV3101) harboring the desired plasmids in the following combination: *pTaARF6*::*LUC* + *pUC18-35S* (empty vector), *pTaARF6*::*LUC* + *35S*::*TaSPL8*, *pTaD2*::*LUC* + *pUC18-35S* (empty vector), and *pTaD2*::*LUC* + *35S*::*TaSPL8*. The activities of firefly luciferase under the control of the *TaARF6* (*pTaARF6*::*LUC*) or *TaD2* (*pTaD2*::*LUC*) promoter and Renilla reniformis under the control of the 35S promoter (*35S*::*REN*) were quantified using the Dual-Luciferase Reporter Assay system (Promega) with the Synergy 2 Multi-Detection Microplate Reader (BioTek Instruments). Normalized data are presented as the ratio of luminescent signal intensity for the pTaARF6::LUC or pTaD2::LUC reporter and luminescent signal intensity for the internal control reporter 35S::REN from three independent biological samples.

Western Blot

Harvested leaves were ground in liquid nitrogen and proteins were extracted with 4× loading buffer (200 mM of Tris-HCl at pH 6.8, 40% [v/v] glycerol, 8% [w/v] SDS, and 20% [v/v] β-mercaptoethanol) at 100°C for 5 min. The solution was placed on ice for 5 min and centrifuged for 10 min at 12,000*g* at room temperature. Protein extracts were separated on 10% (v/v) SDS-PAGE and transferred to a polyvinylidene fluoride membrane (cat. no. 162-0177; Bio-Rad) for 60 min at 300 mA in temperature-controlled conditions. The membrane was blocked using 5% (w/v) defatted milk for 1 h. The membrane and primary antibody (1:1,000), dissolved in 5% (w/v) defatted milk and 1×Tris-buffered saline plus TWEEN 20 (TBST; 1×TBS with 0.1% [v/v] TWEEN 20), were incubated at 4°C overnight. After washing three times for 10 min with 1×TBST, the secondary antibody (1:3,000) was added in 5% (w/v) defatted milk-1×TBST solution and incubated for 1 h at room temperature, followed by three washing steps of 10 min with 1×TBST. Two-component reagent-clarity western ECL Substrate (cat. no. 170-5060; Bio-Rad) was used for detection. The signal was detected with x-ray film.

RNA-Seq

Total RNA was isolated as reported above for RT-qPCR analysis. The lamina joint from *TaSPL8-2A/2B/2d* mutant and LC10, and the corresponding part between the leaf blade and sheath from the *TaSPL8-2a/2b/2d* mutant at the heading stage, were collected. Three replicates of 10 plants each were used for each tissue type. Barcoded cDNA libraries were constructed using Poly-A Purification TruSeq library reagents (Illumina) and sequenced on HiSeq 2500 or NovaSeq platforms (Illumina). Approximately 10 Gb of high-quality 125-bp or 150-bp paired-end reads were generated from each library. The overall sequencing quality of the reads in each sample was evaluated with the software FastQC (v0.11.5; http://www.bioinformatics.babraham.ac.uk). Poor-quality bases were removed using Trimmomatic (v0.36; Bolger et al., 2014) in its paired-end model with the parameters "LEADING:3 TRAILING:3 HEADCROP:6 SLIDINGWINDOW:4:15 MINLEN:40." The remaining reads were aligned to the wheat reference genome sequence IWGSCv1 (http://www.wheatgenome.org/) using the software TopHat2 v2.11 (https://ccb.jhu.edu/software/tophat/index.shtml) with the parameters "–b2-D 20–b2-R 3 -N 3–read-edit-dist 3" (Kim et al., 2013), and only the uniquely mapped reads were retained for the following analysis. The tool FeatureCounts (v1.5.2; http://subread.sourceforge.net/) with the parameters "–readExtension5 70–readExtension3 70 –p –C –s 0" was used to estimate the number of reads mapped to respective high-confidence genes annotated from IWGSCv1 in each sample. The Bioconductor package "DESeq2" (Love et al., 2014) was used to perform differential expression analysis between *TaSPL8* mutant lines and the wild type, and only the genes with an absolute value of $\log_2$ (fold change) ≥ 1 and P value < 0.05 were considered as DEGs.

For GO analysis, cDNAs of high-confidence genes were aligned to the protein sequences of *Oryza sativa* and Arabidopsis (*Arabidopsis thaliana*) using the program BLASTX (https://blast.ncbi.nlm.nih.gov/Blast.cgi?LINK_LOC=blasthome&PAGE_TYPE=BlastSearch&PROGRAM=blastx) with an e-value cutoff of 1e-05. Only the best alignment with identity ≥ 50% and aligned length ≥ 30 amino acids were considered. GO annotations were obtained based on the orthologs with the priority: *O. sativa* > Arabidopsis. GO enrichment analysis of DEGs was implemented using the GOseq "R" package (https://www.rdocumentation.org/packages/goseq/versions/1.24.0/topics/goseq), which is based on the Wallenius noncentral hypergeometric distribution and can adjust for gene length bias (Young et al., 2010). GO terms with false discovery rate < 0.01 were considered as statistically significantly enriched.

EMSA

The full-length ORF sequence of *TaSPL8* was cloned into the *Bam*HI site of the pGEX6P-1 vector to produce the chimeric GST-TaSPL8 protein (primer sequences are listed in Supplemental Table S5). Expression of recombinant protein in Transetta (DE3) *Escherichia coli* (TransGen, Beijing) was induced with 0.1 mM of isopropyl-B-D-thiogalactopyranoside in Luria Bertani buffer overnight at 16°C. Cells were subsequently harvested, washed, and suspended in 30 mL of phosphate-buffered saline (137 mM of NaCl, 2.7 mM of KCl, 10 mM OF Na_2HPO_4, and 2 mM of KH_2PO_4) containing 1 mM of PMSF and 1/2 a tablet of protease inhibitor cocktail (Roche). Then, cells were sonicated for 30 min and centrifuged at 13,000*g* for 45 min at 4°C. The supernatant was filtered through a 0.22-μm membrane into a 50-mL tube. The supernatant was mixed with 1 mL of GST MAG Agarose Beads (Novagen) and shaken overnight at 4°C. GST beads were washed four times with 5 mL of phosphate-buffered saline and the recombinant proteins were eluted by incubation at 4°C for more than 4 h with 50 mM of Tris-HCl at pH 8.0 supplemented with 10 mM of reduced glutathione. Protein concentration was determined using a NanoDrop 2000 spectrophotometer (Thermo Fisher Scientific).

The biotin-probe was 5′ end-labeled with biotin. Double-stranded oligonucleotides used in the assays were annealed by cooling from 100°C to room temperature in annealing buffer (Guo et al., 2018). DNA-binding reactions were performed in 20 μL of 1×binding buffer (100 mM OF Tris, 500 mM of KCl, and 10 mM of dithiothreitol at pH 7.5), 10% (v/v) glycerol, 0.5 mM of EDTA, 10 mM of $ZnCl_2$, and 50-ng μL^{-1} poly dI-dC (Thermo Scientific). Competition analysis was done by adding 5- and 10- fold molar excess of the unlabeled DNA fragment (same sequence used for the labeled probe) to the binding reaction, 5 min before the labeled probe. After incubation at room temperature for 30 min, samples were loaded onto a 6% native polyacrylamide gel. Electrophoretic transfer to a nylon membrane and detection of the biotin-labeled DNA was performed with the Light Shift Chemiluminescent EMSA Kit (Thermo Fisher Scientific) according to the manufacturer's instructions.

Quantification of Endogenous IAA and BR

The lamina joint of the wild type and the *TaSPL8-2a/2b/2d* line were harvested at the heading stage. Quantification of endogenous IAA and BR were performed as described in Chen et al. (2012) and Ding et al. (2013). Each experiment was performed using three replicates.

Statistical Analysis

The statistical analyses, including Student's *t* test and correlation, were performed with the software SPSS v21 (SPSS/IBM). All barcharts and boxplot results were graphically presented using the software Prism v6.0 (GraphPad).

Phylogenetic Analysis

For phylogenetic analysis, related protein sequences to TaARF6 and TaD2 in Arabidopsis and rice were selected by employing a National Center for Biotechnology Information (NCBI) BLASTp search (https://blast.ncbi.nlm.nih.gov/Blast.cgi?PAGE=Proteins) using the nonredundant protein sequences database. Their corresponding accession numbers were shown in Supplemental Figure S6. The phylogenetic tree was generated by the "neighbor joining tree" method in MEGA5 software.

Primers for RT-qPCR and Vector Construction

All primers used in this research are listed in Supplemental Table S5.

Accession Numbers

Accession code: the genomic DNA sequence of *TaSPL8* in LC10 has been deposited in GenBank with the accession no. MH765574. *AUXIN RESPONSE FACTOR TaARF6* gene: TraesCS5B01G039800.1; *CYP90D2 TaD2* gene: TraesCS3A01G103800.

RNA sequencing data are available at the NCBI Sequence Read Archive (http://www.ncbi.nlm.nih.gov/sra) under accession no. SRP157960.

Supplemental Data

The following supplemental materials are available.

Supplemental Figure S1. Schematic of genotype of LC10, *cpa*, NIL^{LC10}, and NIL^{cpa}.

Supplemental Figure S2. A fragment on chromosome 2D was deleted in the *cpa* mutant.

Supplemental Figure S3. CRISPR/Cas9 knock-out *TaSPL8* mutants in CB037 and Bobwhite cultivars.

Supplemental Figure S4. Heat map for the DEGs involved in auxin and BR signaling and cell elongation in the wild type and *TaSPL8* mutants.

Supplemental Figure S5. TaSPL8 in vitro binding of sequences containing the GTAC motif.

Supplemental Figure S6. Phylogenetic tree of TraesCS5B01G039800.1 (TaARF6) and TraesCS3A01G103800.1 (TaD2) with Arabidopsis or rice proteins.

Supplemental Figure S7. The phenotypes of *TaSPL8-Myc* overexpression (OE) and wild-type CB037 lines.

Supplemental Table S1. Morphological characterization of wild type and KO-2-1 (*TaSPL8-2a/2b/2d*) mutant plants.

Supplemental Table S2. The names and geographical origins of all wheat cultivars used in this research.

Supplemental Table S3. Differentially expressed transcripts in the *Taspl8-2a/2b/2d* mutant and the wild type in lamina joint tissue.

Supplemental Table S4. Differentially expressed transcripts in the *Taspl8-2A/2B/2d* mutant and the wild type in lamina joint tissue.

Supplemental Table S5. Primers and Gene IDs for sequences used in this study.

ACKNOWLEDGMENTS

We thank Dr. Qijun Chen (China Agricultural University), Dr. Rentao Song (China Agricultural University), and Dr. Xingguo Ye (Chinese Academy of Agricultural Sciences) for providing the CRISPR-Cas9 vector (pBUE11), the transient expression vectors (pUC18-35S and pGreenII 0800-LUC), and the overexpression vector (pMWB122), respectively. We thank Prof. Mingcheng Luo (University of California, Davis) for providing the *A. tauschii* genome sequence. We thank Prof. Guihua Bai (Kansas State University) for critical reading of the article. We thank Dr. Yuqi Feng (Wuhan University) for assistance in IAA and BR quantification and Dr. Hongxia Li and Dr. Yu Wang (Northwest A&F University) for help in phenotypic measurements of yield-related traits. We also thank the International Wheat Genome Sequencing Consortium for providing the wheat reference sequence.

Received February 28, 2019; accepted June 4, 2019; published June 17, 2019.

LITERATURE CITED

Appels R, Eversole K, Feuillet C, Keller B, Rogers J, Stein N, Pozniak CJ, Stein N, Choulet F, Distelfeld A, et al (2018) Shifting the limits in wheat research and breeding using a fully annotated reference genome. Science **361:** eaar7191

Austin R, Ford M, Edrich J, Hooper B (1976) Some effects of leaf posture on photosynthesis and yield in wheat. Ann Appl Biol **83:** 425–446

Bai F, Reinheimer R, Durantini D, Kellogg EA, Schmidt RJ (2012) TCP transcription factor, BRANCH ANGLE DEFECTIVE 1 (BAD1), is required for

normal tassel branch angle formation in maize. Proc Natl Acad Sci USA **109:** 12225–12230

Bai MY, Zhang LY, Gampala SS, Zhu SW, Song WY, Chong K, Wang ZY (2007) Functions of OsBZR1 and 14-3-3 proteins in brassinosteroid signaling in rice. Proc Natl Acad Sci USA **104:** 13839–13844

Bian H, Xie Y, Guo F, Han N, Ma S, Zeng Z, Wang J, Yang Y, Zhu M (2012) Distinctive expression patterns and roles of the miRNA393/TIR1 homolog module in regulating flag leaf inclination and primary and crown root growth in rice (*Oryza sativa*). New Phytol **196:** 149–161

Bolger AM, Lohse M, Usadel B (2014) Trimmomatic: A flexible trimmer for Illumina sequence data. Bioinformatics **30:** 2114–2120

Cao H, Chen S (1995) Brassinosteroid-induced rice lamina joint inclination and its relation to indole-3-acetic acid and ethylene. Plant Growth Regul **16:** 189–196

Chen ML, Fu XM, Liu JQ, Ye TT, Hou SY, Huang YQ, Yuan BF, Wu Y, Feng YQ (2012) Highly sensitive and quantitative profiling of acidic phytohormones using derivatization approach coupled with nano-LC-ESI-Q-TOF-MS analysis. J Chromatogr B Analyt Technol Biomed Life Sci **905:** 67–74

Cosgrove DJ (2015) Plant expansins: Diversity and interactions with plant cell walls. Curr Opin Plant Biol **25:** 162–172

Ding J, Mao LJ, Wang ST, Yuan BF, Feng YQ (2013) Determination of endogenous brassinosteroids in plant tissues using solid-phase extraction with double layered cartridge followed by high-performance liquid chromatography-tandem mass spectrometry. Phytochem Anal **24:** 386–394

Donald CM (1968) The breeding of crop ideotypes. Euphytica **17:** 385–403

Dong H, Zhao H, Li S, Han Z, Hu G, Liu C, Yang G, Wang G, Xie W, Xing Y (2018) Genome-wide association studies reveal that members of bHLH subfamily 16 share a conserved function in regulating flag leaf angle in rice (*Oryza sativa*). PLoS Genet **14:** e1007323

Du H, Wu N, Fu J, Wang S, Li X, Xiao J, Xiong L (2012) A GH3 family member, OsGH3-2, modulates auxin and abscisic acid levels and differentially affects drought and cold tolerance in rice. J Exp Bot **63:** 6467–6480

Duvick D (2005) Genetic progress in yield of United States maize (*Zea mays* L.). Maydica **50:** 193–202

El Baidouri M, Murat F, Veyssiere M, Molinier M, Flores R, Burlot L, Alaux M, Quesneville H, Pont C, Salse J (2017) Reconciling the evolutionary origin of bread wheat (*Triticum aestivum*). New Phytol **213:** 1477–1486

Feldman M, Levy AA, Fahima T, Korol A (2012) Genomic asymmetry in allopolyploid plants: Wheat as a model. J Exp Bot **63:** 5045–5059

Guan Q, Yue X, Zeng H, Zhu J (2014) The protein phosphatase RCF2 and its interacting partner NAC019 are critical for heat stress-responsive gene regulation and thermotolerance in Arabidopsis. Plant Cell **26:** 438–453

Guo G, Liu X, Sun F, Cao J, Huo N, Wuda B, Xin M, Hu Z, Du J, Xia R, et al (2018) Wheat miR9678 affects seed germination by generating phased siRNAs and modulating abscisic acid/gibberellin signaling. Plant Cell **30:** 796–814

Hellens RP, Allan AC, Friel EN, Bolitho K, Grafton K, Templeton MD, Karunairetnam S, Gleave AP, Laing WA (2005) Transient expression vectors for functional genomics, quantification of promoter activity and RNA silencing in plants. Plant Methods **1:** 13

Hong Z, Ueguchi-Tanaka M, Shimizu-Sato S, Inukai Y, Fujioka S, Shimada Y, Takatsuto S, Agetsuma M, Yoshida S, Watanabe Y, et al (2002) Loss-of-function of a rice brassinosteroid biosynthetic enzyme, C-6 oxidase, prevents the organized arrangement and polar elongation of cells in the leaves and stem. Plant J **32:** 495–508

Hong Z, Ueguchi-Tanaka M, Umemura K, Uozu S, Fujioka S, Takatsuto S, Yoshida S, Ashikari M, Kitano H, Matsuoka M (2003) A rice brassinosteroid-deficient mutant, *ebisu dwarf* (*d2*), is caused by a loss of function of a new member of cytochrome P450. Plant Cell **15:** 2900–2910

Ishida Y, Tsunashima M, Hiei Y, Komari T (2015) Wheat (*Triticum aestivum* L.) transformation using immature embryos. Methods Mol Biol **1223:** 189–198

Ishii T, Numaguchi K, Miura K, Yoshida K, Thanh PT, Htun TM, Yamasaki M, Komeda N, Matsumoto T, Terauchi R, et al (2013) OsLG1 regulates a closed panicle trait in domesticated rice. Nat Genet **45:** 462–465, e1–e2

Isidro J, Knox R, Clarke F, Singh A, DePauw R, Clarke J, Somers D (2012) Quantitative genetic analysis and mapping of leaf angle in durum wheat. Planta **236:** 1713–1723

Jang S, An G, Li HY (2017) Rice leaf angle and grain size are affected by the OsBUL1 transcriptional activator complex. Plant Physiol **173:** 688–702

Johnston R, Wang M, Sun Q, Sylvester AW, Hake S, Scanlon MJ (2014) Transcriptomic analyses indicate that maize ligule development recapitulates gene expression patterns that occur during lateral organ initiation. Plant Cell **26:** 4718–4732

Kim D, Pertea G, Trapnell C, Pimentel H, Kelley R, Salzberg SL (2013) TopHat2: Accurate alignment of transcriptomes in the presence of insertions, deletions and gene fusions. Genome Biol **14:** R36

Komatsu K, Maekawa M, Ujiie S, Satake Y, Furutani I, Okamoto H, Shimamoto K, Kyozuka J (2003) LAX and SPA: Major regulators of shoot branching in rice. Proc Natl Acad Sci USA **100:** 11765–11770

Kong F, Zhang T, Liu J, Heng S, Shi Q, Zhang H, Wang Z, Ge L, Li P, Lu X, et al (2017) Regulation of leaf angle by auricle development in maize. Mol Plant **10:** 516–519

Kropat J, Tottey S, Birkenbihl RP, Depège N, Huijser P, Merchant S (2005) A regulator of nutritional copper signaling in Chlamydomonas is an SBP domain protein that recognizes the GTAC core of copper response element. Proc Natl Acad Sci USA **102:** 18730–18735

Lau S, Jürgens G, De Smet I (2008) The evolving complexity of the auxin pathway. Plant Cell **20:** 1738–1746

Lauer S, Hall BD, Mulaosmanovic E, Anderson SR, Nelson B, Smith S (2012) Morphological changes in parental lines of pioneer brand maize hybrids in the U.S. central corn belt. Crop Sci **52:** 1033–1043

Lee EA, Tollenaar M (2007) Physiological basis of successful breeding strategies for maize grain yield. Crop Sci **47:** S202–S215

Lee J, Park J-J, Kim SL, Yim J, An G (2007) Mutations in the rice liguleless gene result in a complete loss of the auricle, ligule, and laminar joint. Plant Mol Biol **65:** 487–499

Lewis MW, Bolduc N, Hake K, Htike Y, Hay A, Candela H, Hake S (2014) Gene regulatory interactions at lateral organ boundaries in maize. Development **141:** 4590–4597

Li D, Wang L, Wang M, Xu YY, Luo W, Liu YJ, Xu ZH, Li J, Chong K (2009) Engineering *OsBAK1* gene as a molecular tool to improve rice architecture for high yield. Plant Biotechnol J **7:** 791–806

Li H, Jiang L, Youn JH, Sun W, Cheng Z, Jin T, Ma X, Guo X, Wang J, Zhang X, et al (2013) A comprehensive genetic study reveals a crucial role of CYP90D2/D2 in regulating plant architecture in rice (*Oryza sativa*). New Phytol **200:** 1076–1088

Liu K, Li Y, Chen X, Li L, Liu K, Zhao H, Wang Y, Han S (2018a) ERF72 interacts with ARF6 and BZR1 to regulate hypocotyl elongation in Arabidopsis. J Exp Bot **69:** 3933–3947

Liu K, Xu H, Liu G, Guan P, Zhou X, Peng H, Yao Y, Ni Z, Sun Q, Du J (2018b) QTL mapping of flag leaf-related traits in wheat (*Triticum aestivum L.*). Theor Appl Genet **131:** 839–849

Liu S, Yeh CT, Tang HM, Nettleton D, Schnable PS (2012) Gene mapping via bulked segregant RNA-Seq (BSR-Seq). PLoS One **7:** e36406

López-Bucio J, Hernández-Abreu E, Sánchez-Calderón L, Nieto-Jacobo MF, Simpson J, Herrera-Estrella L (2002) Phosphate availability alters architecture and causes changes in hormone sensitivity in the Arabidopsis root system. Plant Physiol **129:** 244–256

Love MI, Huber W, Anders S (2014) Moderated estimation of fold change and dispersion for RNA-seq data with DESeq2. Genome Biol **15:** 550

Luo MC, Gu YQ, Puiu D, Wang H, Twardziok SO, Deal KR, Huo N, Zhu T, Wang L, Wang Y, et al (2017) Genome sequence of the progenitor of the wheat D genome *Aegilops tauschii*. Nature **551:** 498–502

Luo X, Zheng J, Huang R, Huang Y, Wang H, Jiang L, Fang X (2016) Phytohormones signaling and crosstalk regulating leaf angle in rice. Plant Cell Rep **35:** 2423–2433

Mantilla-Perez MB, Salas Fernandez MG (2017) Differential manipulation of leaf angle throughout the canopy: Current status and prospects. J Exp Bot **68:** 5699–5717

Moreno MA, Harper LC, Krueger RW, Dellaporta SL, Freeling M (1997) liguleless1 encodes a nuclear-localized protein required for induction of ligules and auricles during maize leaf organogenesis. Genes Dev **11:** 616–628

Nagpal P, Ellis CM, Weber H, Ploense SE, Barkawi LS, Guilfoyle TJ, Hagen G, Alonso JM, Cohen JD, Farmer EE, et al (2005) Auxin response factors ARF6 and ARF8 promote jasmonic acid production and flower maturation. Development **132:** 4107–4118

Ning J, Zhang B, Wang N, Zhou Y, Xiong L (2011) Increased leaf angle1, a Raf-like MAPKKK that interacts with a nuclear protein family, regulates mechanical tissue formation in the Lamina joint of rice. Plant Cell **23:** 4334–4347

Oh E, Zhu J-Y, Bai M-Y, Arenhart RA, Sun Y, Wang Z-Y (2014) Cell elongation is regulated through a central circuit of interacting transcription factors in the Arabidopsis hypocotyl. eLife **3:** e03031

Pacheco-Villalobos D, Díaz-Moreno SM, van der Schuren A, Tamaki T, Kang YH, Gujas B, Novak O, Jaspert N, Li Z, Wolf S, et al (2016) The effects of high steady state auxin levels on root cell elongation in brachypodium. Plant Cell **28:** 1009–1024

Pendleton JW, Smith GE, Winter SR, Johnston TJ (1968) Field investigations of the relationships of leaf angle in corn (*Zea mays L.*) to grain yield and apparent photosynthesis1. Agron J **60:** 422–424

Ruan W, Guo M, Xu L, Wang X, Zhao H, Wang J, Yi K (2018) An SPX-RLI1 module regulates leaf inclination in response to phosphate availability in rice. Plant Cell **30:** 853–870

Sakamoto T, Morinaka Y, Ohnishi T, Sunohara H, Fujioka S, Ueguchi-Tanaka M, Mizutani M, Sakata K, Takatsuto S, Yoshida S, et al (2006) Erect leaves caused by brassinosteroid deficiency increase biomass production and grain yield in rice. Nat Biotechnol **24:** 105–109

Sakamoto T, Morinaka Y, Inukai Y, Kitano H, Fujioka S (2013) Auxin signal transcription factor regulates expression of the brassinosteroid receptor gene in rice. Plant J **73:** 676–688

Sénéchal F, Wattier C, Rustérucci C, Pelloux J (2014) Homogalacturonan-modifying enzymes: Structure, expression, and roles in plants. J Exp Bot **65:** 5125–5160

Sinclair TR, Sheehy JE (1999) Erect leaves and photosynthesis in rice. Science **283:** 1455

Tanaka A, Nakagawa H, Tomita C, Shimatani Z, Ohtake M, Nomura T, Jiang C-J, Dubouzet JG, Kikuchi S, Sekimoto H, et al (2009) BRASSINOSTEROID UPREGULATED1, encoding a helix-loop-helix protein, is a novel gene involved in brassinosteroid signaling and controls bending of the lamina joint in rice. Plant Physiol **151:** 669–680

Wada K, Marumo S, Ikekawa N, Morisaki M, Mori K (1981) Brassinolide and homobrassinolide promotion of lamina inclination of rice seedlings. Plant Cell Physiol **22:** 323–325

Wang K, Liu H, Du L, Ye X (2017) Generation of marker-free transgenic hexaploid wheat via an Agrobacterium-mediated co-transformation strategy in commercial Chinese wheat varieties. Plant Biotechnol J **15:** 614–623

Wang X, Zhang H, Li Y, Zhang Z, Li L, Liu B (2016) Transcriptome asymmetry in synthetic and natural allotetraploid wheats, revealed by RNA-sequencing. New Phytol **209:** 1264–1277

Wu Q, Chen Y, Fu L, Zhou S, Chen J, Zhao X, Zhang D, Ouyang S, Wang Z, Li D, et al (2015) QTL mapping of flag leaf traits in common using an integrated high-density SSR and SNP genetic linkage map. Euphytica **208:** 337–351

Xing HL, Dong L, Wang ZP, Zhang HY, Han CY, Liu B, Wang XC, Chen QJ (2014) A CRISPR/Cas9 toolkit for multiplex genome editing in plants. BMC Plant Biol **14:** 327

Yamamuro C, Ihara Y, Wu X, Noguchi T, Fujioka S, Takatsuto S, Ashikari M, Kitano H, Matsuoka M (2000) Loss of function of a rice brassinosteroid insensitive1 homolog prevents internode elongation and bending of the lamina joint. Plant Cell **12:** 1591–1606

Yang H, Liu X, Xin M, Du J, Hu Z, Peng H, Rossi V, Sun Q, Ni Z, Yao Y (2016) Genome-wide mapping of targets of maize histone deacetylase HDA101 reveals its function and regulatory mechanism during seed development. Plant Cell **28:** 629–645

Young MD, Wakefield MJ, Smyth GK, Oshlack A (2010) Gene ontology analysis for RNA-seq: Accounting for selection bias. Genome Biol **11:** R14

Zhang L-Y, Bai M-Y, Wu J, Zhu J-Y, Wang H, Zhang Z, Wang W, Sun Y, Zhao J, Sun X, et al (2009) Antagonistic HLH/bHLH transcription factors mediate brassinosteroid regulation of cell elongation and plant development in rice and Arabidopsis. Plant Cell **21:** 3767–3780

Zhang S, Wang S, Xu Y, Yu C, Shen C, Qian Q, Geisler M, Jiang A, Qi Y (2015) The auxin response factor, OsARF19, controls rice leaf angles through positively regulating OsGH3-5 and OsBRI1. Plant Cell Environ **38:** 638–654

Zhao S-Q, Hu J, Guo L-B, Qian Q, Xue H-W (2010) Rice leaf inclination2, a VIN3-like protein, regulates leaf angle through modulating cell division of the collar. Cell Res **20:** 935–947

Zhao S-Q, Xiang J-J, Xue H-W (2013) Studies on the rice LEAF INCLINATION1 (LC1), an IAA-amido synthetase, reveal the effects of auxin in leaf inclination control. Mol Plant **6:** 174–187

Zhou LJ, Xiao LT, Xue HW (2017) Dynamic cytology and transcriptional regulation of rice lamina joint development. Plant Physiol **174:** 1728–1746

Zhu Z, Tan L, Fu Y, Liu F, Cai H, Xie D, Wu F, Wu J, Matsumoto T, Sun C (2013) Genetic control of inflorescence architecture during rice domestication. Nat Commun **4:** 2200